Valuing Credit Default Swaptions with Stochastic Intensity Models

Andreas Roti
Master's Thesis, MSc. Finance

Supervisor: Thomas Kokholm
Department of Economics and Business

Aarhus University
School of Business and Social Science
August 2013

Content

1 Introduction

Stochastic intensity models are commonly used in credit risk modeling, partly attractive due to the easy calibration of the model parameters to market data, allowing for the valuation of other derivatives and securities. When calibrating an intensity model to credit default swap market quotes, different parameters might be obtained, providing an equally good fit to the market. Whether or not these different parameters provide an equally good fit when it comes to valuing credit default swaptions, an option to enter a credit default swap, is less clear. This thesis uses this as a starting point to set out and investigate the *suitability of using stochastic intensity models calibrated to credit default swap data when valuing credit default swaptions*. The performances of three different stochastic intensity models will be studied; the CIR model, the Gamma Ornstein-Uhlenbeck model and the Inverse Gaussian Ornstein-Uhlenbeck model. While the CIR model is the most common stochastic intensity model in the credit risk literature, the Gamma- and Inverse Gaussian Ornstein-Uhlenbeck models are more recently introduced to credit risk modeling.

The models will be examined in three different aspects. Firstly, the different parameters obtained in the calibration of a model will be compared. The occurrence of finding different parameters in the calibration of an intensity model depends mostly on initiating the calibration procedure with different starting values. By carefully selecting an interval for the parameters, and search for solutions with different combinations of starting values within this interval, different fitted parameters will be obtained. Secondly, the corresponding credit default swaption prices estimated with the use of these different parameters will be analyzed, both in terms of the specific model's features in credit default swap valuation and the difference between the values estimated for different parameters. Lastly, the models will be further investigated through the implied volatilities generated by the estimated credit default swaption values.

This thesis is structured as follows: section 2 introduces the credit derivatives relevant for the analysis, before section 3 addresses the general approaches to modeling credit risk. Section 4 takes a closer look at the intensity models of interest, where their different properties are highlighted. Section 5 presents the procedure of valuing credit default swaptions, under two different sets of assumptions. Section 6 explains the methodology used to perform the analysis, followed by the results in section 7. Finally, section 8 concludes the thesis.

2 Credit Derivatives

A credit derivative can be defined as a derivative where the payoff is conditioned on a *credit event*. A credit event is the term often used for the default of an obligor (Schönbucher, 2003, p.8). The International Swaps and Derivatives Association (ISDA) has been an important driver of the growth in the credit derivatives market, enhancing the efficiency and safety through standardization. The standard ISDA (2003) definition of a credit event covers the inclusion of one or more of the following events:

- Bankruptcy
- Failure to pay
- Obligation acceleration
- Obligation default
- Repudiation/moratorium
- Restructuring

These are the standard events, but the parties in a contract can agree to exclude one or more of them. In this thesis, the terms credit event and default will be used interchangeably.

Credit derivatives can be used for different purposes; hedging, investing, speculating or to satisfy regulatory demands. Through credit derivatives it is simple to hedge existing credit exposure by going short in credit risk. Especially for banks, where credit risk historically has resided on bank loan books, credit derivatives have worked as a mean for shifting this risk into the capital markets. The unfunded nature of most credit derivatives attracts investors as a cheaper alternative to buying cash bonds (O'Kane, 2008, pp. 1-2). Since the buyer of a credit derivative is not required to own any of the obligor's debt, they may be used to speculate on the future prospects of the obligor, something that further enhances the liquidity (French et al. 2010).

2.1 Credit Default Swap

The most common credit derivative is the credit default swap, hereafter named CDS. A CDS is a contract that provides protection against losses caused by a default of a specific entity, named the *reference entity.* A plain CDS-contract can be described as follows: a contract is agreed upon between two parties, a buyer of protection and a seller of protection. The buyer pays the seller periodic payments on predetermined payment dates, up until the reference entity defaults or the CDS-contract matures. These payments are called *premium payments*. In return the seller pays the buyer a *protection payment* if the reference entity defaults during the life of the CDS-contract.

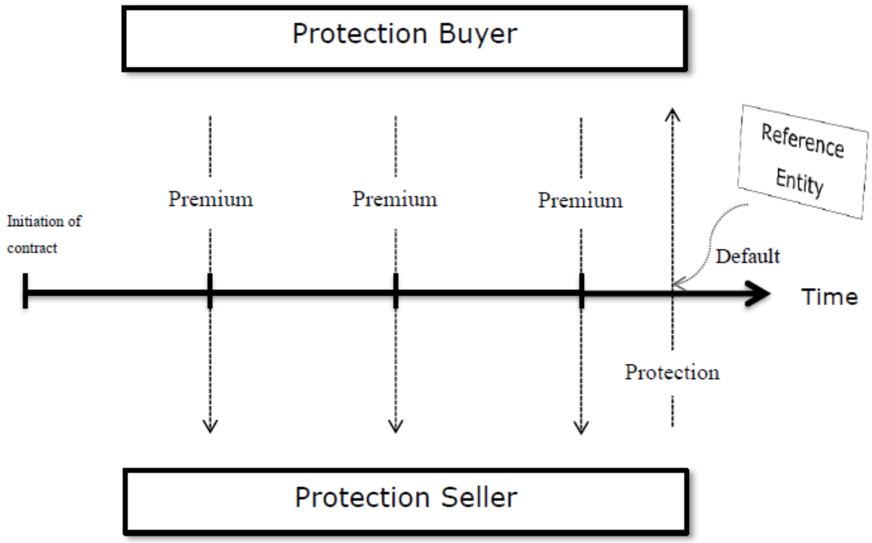

Figure 2.1: *Example of the cash flows between the two parties in a CDS. In this scenario, the reference entity defaults and this triggers the protection payment from the protection seller.*

The exercise of valuing a credit default swap is to find the present value of the stream of future uncertain payments associated with the contract. On the protection buyer side there are premium payments which are only paid as long as no default of the reference entity has occurred, while on the protection seller side the payment is only paid in the case of default. These claims can be valued using the well-known concept of risk-neutral valuation, which is refreshed in the next subsection.

2.1.1 Risk-Neutral Valuation

The concept of risk-neutral valuation was first introduced by Black & Scholes (1973) and Merton (1973). This later motivated a study by Harrison & Pliska (1981) where they showed that, under some technical conditions, with the absence of arbitrage opportunities the real probability measure $\boldsymbol{P}$ which can be replaced with an equivalent martingale measure $\boldsymbol{Q}$. Under this probability measure $\boldsymbol{Q}$, the discounted price of an asset is a martingale. The discount factor is the riskless asset, and the probability measure $\boldsymbol{Q}$ is often referred to as the risk-neutral probability measure. This change of measure can also be seen as a result of risk aversion, where one can give more weight to unfavorable outcomes and less weight to favorable ones (Delbaen & Schachermayer, 1994). Define the riskless asset as:

$$S_t = e^{\int_0^t r(s)ds} \quad \textbf{2.1}$$

Where $r(t)$ is the continuously compounded risk-free rate at time t. The value of a contingent claim at time t, V_t, that pays off V_T at time $T > t$ can be found through:

$$\frac{V_t}{S_t} = \mathbb{E}_t^Q\left[\frac{V_T}{S_T}\right]$$

where $\mathbb{E}_t^Q[\cdot]$ denotes the expectation operator associated with $\boldsymbol{Q}$, based on all information at time t. We rearrange and write:

$$V_t = \mathbb{E}_t^Q\left[\frac{S_t}{S_T}V_T\right] \quad \textbf{2.2}$$

Now consider a contingent claim that at time T pays off 1 in case of no default, and 0 in the case of default by an entity. Denote τ as the time of default. By assuming that the risk-free rate is a constant r, the time t value of such a claim can through (2.2) be expressed as:

$$V_t = e^{-r(T-t)}\mathbb{E}_t^Q\left[1_{\{\tau>T\}}\right] \quad \textbf{2.3}$$

Where

$$1_{\{\tau>T\}} = \begin{cases} 1 \; if \; \tau > T \\ 0 \; if \; \tau \leq T \end{cases}$$

Define the *risk-neutral survival probability* as the probability under the risk-neutral measure of the survival of an entity through time T, conditioned on its survival at time t and all other market information at time t. Denote this probability as:

$$Q_t(\tau > T | \tau > t) \equiv Q(t,T) \quad \textbf{2.4}$$

Using (2.4) the expectation in (2.3) can be expressed as:

$$\mathbb{E}_t^Q\left[1_{\{\tau>T\}}\right] = Q(t,T) \cdot 1 + \big(1 - Q(t,T)\big) \cdot 0 = Q(t,T)$$

Finally, define the time t value of risk-free zero coupon bond that pays out 1 with certainty at time T as:

$$Z(t,T) = e^{-r(T-t)}$$

By combining all this, the value of the claim can be written as:

$$V_t = Z(t,T)Q(t,T) \tag{2.5}$$

This shows that the value of such contingent claims can be expressed as the value of a risk-free zero coupon bond, times the risk-neutral probability that the claim will be paid. This is the expression we need in order to value the different cash flows in a CDS.

The assumption of a constant risk-free rate is quite strict and not very consistent with reality. The risk-neutral valuation method can also be used in the case of both time varying, and stochastic interest rates. Also correlation between the interest rate and, say, an intensity process, can be incorporated. However, as the focus of this thesis is on intensity models, the simplifying assumption of a constant risk-free rate will be made in order to derive nice and clean expressions where the intensity models can easily be employed.

2.1.2 Premium Leg

Now, let us go more in to detail of how a simple CDS contract is structured. Consider a CDS initiated and starting at time *t* and maturing at time T_N with payment dates $T_1, T_2, \dots., T_N$ and an annual premium denoted S^{CDS}. The premium, also called the *spread*, is quoted as a percentage of the par value of debt insured through the contract, typically named the *notional amount*. Define $\delta_i = T_i - T_{i-1}$ as the time between payment dates, measured in years. For a contract with a notional amount equal to 1, the premium payment at time T_i is:

$$\delta_i S^{CDS}$$

The premium will only be paid if the reference entity has not defaulted at time T_i. As was argued in the previous section, we can under the assumption of no arbitrage use equation (2.5) and write the time t value of this claim as:

$$Z(t,T_i)Q(t,T_i)\delta_i S^{CDS}$$

The present value at time t of all premium payments is simply the sum of all these uncertain payments:

$$\sum_{i=1}^{N} Z(t,T_i)Q(t,T_i)\delta_i S^{CDS} \tag{2.6}$$

So far, the concept of *accrued premiums* has not been considered. It is not likely that the reference entity defaults exactly at one of the premium payment dates, it's more likely to default in-between two payment dates. In that case, the protection buyer will be obliged to pay the premium accrued from the previous payment date and the date of default. In reality a very large number of possible accrued premium payments are possible, which complicates calculations. One approach to simplify this, as seen in for instance O'Kane & Turnbull (2003), is to assume that if a default occurs between two payment dates it will on average take place midway between them. The present value of the accrued premiums can then be expressed as:

$$\sum_{i=1}^{N} Z(t,\Delta_i)\, Q_t(T_{i-1} < \tau \le T_i) \frac{\delta_i S^{CDS}}{2} \qquad \textbf{2.7}$$

where $Q_t(T_{i-1} < \tau \le T_i)$ denotes the risk-neutral probability that the reference entity defaults between T_{i-1} and T_i based on all information available at time *t*, and $\Delta_i = \frac{T_{i-1}+T_i}{2}$. By combining (2.4) with the logical argument that the probability of defaulting between $T_{i-1}$and T_i should be equal to the probability of defaulting before T_i minus the probability of defaulting before T_{i-1}, this probability as can be written as:

$$Q_t(T_{i-1} < \tau \le T_i) = Q_t(\tau < T_i | \tau > t) - Q_t(\tau < T_{i-1} | \tau > t)$$
$$Q_t(T_{i-1} < \tau \le T_i) = 1 - Q(t,T_i) - \big(1 - Q(t,T_{i-1})\big)$$
$$Q_t(T_{i-1} < \tau \le T_i) = Q(t,T_{i-1}) - Q(t,T_i)$$

By using this and merging (2.6) and (2.7) an expression for the present value of all possible premium payments, also called the present value of the *premium leg* and denoted by $\Pi^{Prem}(t,T_N,S^{CDS})$, can be written as:

$$\Pi^{Prem}(t,T_N,S^{CDS}) = S^{CDS} \sum_{i=1}^{N} \delta_i \left(Z(t,T_i)Q(t,T_i) + \frac{1}{2} Z(t,\Delta_i)[Q(t,T_{i-1}) - Q(t,T_i)] \right) \qquad \textbf{2.8}$$

Now, as the expression of the value for the cash flows from the buyer of protection in a CDS contract is completed, it is time to derive a similar expression for the cash flow(s) of the seller.

2.1.3 Protection leg

The method of settlement in the case of default for the protection payment is specified when the two parties enter the contract, where the options in a standardized contract are physical settlement or cash settlement. In a physical settlement, the buyer of protection has the right to sell *deliverable obligations* issued by the reference entity to the protection seller for the face value of the debt. In a cash settlement, the protection seller simply pays the protection buyer the difference between the face value of the *reference obligation* and its market value in cash. In a cash settlement the reference obligation is a single bond or loan, and its market value after a default may be determined by polling market participants. (Bonfirm, 2005, ch. 6). This contrasts to a physical settlement where typically several bonds or loans qualify as deliverable obligations. This is preferable as one contract can be used to hedge any of the deliverable obligations, which enhances liquidity. But it also gives the protection buyer a *delivery option*, meaning that the buyer can choose which bonds or loans used to settle the contract. The delivery option has a value at maturity if different deliverable obligations trade at different prices after a default. Its payoff will then be the difference between the value of the security the buyer holds and the cheapest deliverable obligation (O'Kane, 2008). To ease calculations, we assume cash settlement and thereby ignore this delivery option.

The market value of the reference obligation after a default per unit of face value is commonly referred to as the *recovery rate*. The normal practice is to treat the recovery rate independently of the default probability. This assumption is criticized by some as rather simplistic, since empirical evidence shows a relationship between the two (See for instance Altman et. al (2005)). However, in the use of intensity models, credit default swap values seem to be quite insensitive to the recovery rate (See for instance Elizalde (2005)). As a result of this, together with the nice expressions that can be formed, the recovery rate is treated as a constant R.

By assuming cash settlement, and a constant recovery rate R, the protection payment can then be denoted as $(1 - R)$ per notional amount insured. As seen in Houweling & Vorst (2005) and O'Kane & Turnbull (2003), we will assume that default can only happen on a finite number of discrete time points each year. Let M denote this number. The present value of the protection leg, denoted $\Pi^{Prot}(t, T_N)$, can then be written as.

$$\Pi^{Prot}(t, T_N) = (1-R) \sum_{m=1}^{M\times(T_N-t)} Z\big(t, \Upsilon_{t,m,M}\big)\big[Q\big(t, \Upsilon_{t,m-1,M}\big) - Q\big(t, \Upsilon_{t,m,M}\big)\big] \qquad \textbf{2.9}$$

where $\Upsilon_{t,m,M} = t + \frac{m}{M}$.

From this it is clear that a payment at time $\Upsilon_{t,m,M}$ is contingent on a default between $\Upsilon_{t,m-1,M}$ and $\Upsilon_{t,m,M}$.

2.1.4 The Value of a Credit Default Swap and the Fair Spread

The value of a Credit Default Swap, as seen from the protection buyer's side, is what he claims minus what he pays. His claim is the present value of the protection leg, and in return he pays the present value of the premium leg. Let $V(t, T_N, S^{CDS})$ denote the value of a CDS to the protection buyer at time t, maturing at time T_N with an annual spread S^{CDS}. An expression of its value can be found by subtracting (2.8) from (2.9):

$$\begin{aligned} V(t, T_N, S^{CDS}) = (1-R) &\sum_{m=1}^{M\times(T_N-t)} Z\big(t, \Upsilon_{t,m,M}\big)\big[Q\big(t, \Upsilon_{t,m-1,M}\big) - Q\big(t, \Upsilon_{t,m,M}\big)\big] \\ &- S^{CDS} \sum_{i=1}^{N} \delta_i \left(Z(t, T_i) Q(t, T_i) + \frac{1}{2} Z(t, \Delta_i)[Q(t, T_{i-1}) - Q(t, T_i)] \right) \end{aligned} \qquad \textbf{2.10}$$

It usually does not cost anything to enter a credit default swap. If so, the contract has a zero value and the premium and protection leg must have the same value. By setting $V(t, T_N, S^{CDS})$ equal to zero and solving for S^{CDS} the *fair spread*, meaning the spread that secures that the contract is fairly priced, can be expressed as:

$$S^{CDS} = \frac{(1-R) \sum_{m=1}^{M\times(T_N-t)} Z\big(t, \Upsilon_{t,m,M}\big)\big[Q\big(t, \Upsilon_{t,m-1,M}\big) - Q\big(t, \Upsilon_{t,m,M}\big)\big]}{\sum_{i=1}^{N} \delta_i \left(Z(t, T_i) Q(t, T_i) + \frac{1}{2} Z(t, \Delta_i)[Q(t, T_{i-1}) - Q(t, T_i)] \right)} \qquad \textbf{2.11}$$

However, as time moves on the credit quality of the reference entity might change. This will in order change the value of the contract. An improved credit quality will reduce the spread, which intuitively tells us that the contract will have a negative value for the protection buyer as he then pays more than the fair spread in the market for the same protection. Assume that a protection buyer entered a contract some time ago that offers protection against the default on a given reference entity, where he pays an annual spread of S^o. Refer to this contract as the *old contract.* Assume further that a *new contract* with maturity equal to the remaining maturity of the old contract can now be entered at no cost with an annual spread of S^n. Because the new contract has a zero value at initiation, we can write the value of the old contract as:

$$V(t, T_N, S^o) = V(t, T_N, S^o) - V(t, T_N, S^n)$$

When inserting equation (2.10) for the values of the old and the new contract respectively, we end up with the following expression:

$$V(t, T_N, S^o) = (S^n - S^o) \sum_{i=1}^{N} \delta_i \left(Z(t, T_i) Q(t, T_i) + \frac{1}{2} Z(t, \Delta_i) [Q(t, T_{i-1}) - Q(t, T_i)] \right) \quad \textbf{2.12}$$

The clearly shows, as indicated above, that a decrease in the spread relative to the old spread will lead to a negative value for the protection buyer, while an increase in the spread will affect the value of the contract positive. An intuitive way to think of (2.12) is to imagine that the protection buyer enters an offsetting transaction where he sells the new contract at zero cost. The protection leg will then be perfectly hedged, and he will at each payment date until default or maturity receive the new spread S^n and pay the old spread S^o, and the value of the contract is the present value of this stream of payments (O'Kane, 2008, p. 98).

Remark: *The use of equation (2.10) to value an old CDS-contract is only accurate if the valuation takes place on a payment date. If this formula is used to value a CDS in-between payment dates the premium accrued from the previous payment date is ignored.*

2.1.5 Counterparty Credit Risk

The presence of counterparty credit risk has so far been ignored. In terms of a CDS contract, counterparty credit risk refers to the risk that either the protection buyer or protection seller defaults during the life of the contract, and thus fails to honor his obligations (Bomfim, 2005, p. 267). Seen from the protection seller's point of view, a default of the protection buyer will stop the incoming stream of payments of the CDS premium. The protection seller then needs to replace the contract in the market place. If the CDS spread has decreased, the default of the protection buyer will have a cost for the seller, as the premium received for keeping the same level of credit exposure to the reference entity will be lower than before. On the other hand, if the CDS spread has increased, replacing the contract will lead to a gain, due to the higher premium received (O'Kane, 2008, pp. 148-149). The loss to the protection seller due to default of the counterparty is thus limited to the replacement cost of the CDS contract.

However, since a negative market value of the contract to the protection seller means a positive market value of the contract to the protection buyer, a protection buyer on the verge of default will have a strong incentive to sell his part of the contract in the market, realizing the positive market value (Bomfim, 2005). In that case, the default of the original protection buyer will go unnoticed for the protection seller. The exclusion of counterparty credit risk for the protection seller side therefore seems reasonable.

Counterparty credit risk as seen from the side of the protection buyer is more worrying though. If the protection seller defaults before the reference entity, the protection buyer can enter a new contract in the market place, swiftly reinstating the protection. A cost might come in the form of a higher premium however, caused by a deterioration of the reference entity's credit quality from the time of initiation of the original contract. The more severe case occurs should the reference entity and protection seller default within a short period of time, so that the protection seller does not deliver on the protection payment. In that case, the buyer has no chance of reinstating the contract, and the protection payment will be lost. From this, it is clear that the presence of counterparty credit risk depends not only on the credit quality of the protection seller, but also on the presence of default correlation between the reference entity and the protection seller (O'Kane, 2008, pp. 148-149).

Several arrangements are made to mitigate the counterparty credit risk, for instance collateralization agreements and trading through central clearing houses. In addition, it seems logical from the previous discussion that protection buyers would not enter agreements with protection sellers that are likely to default themselves, or that has a high default correlation with the reference entity in question. Despite of this, counterparty credit risk is still present, as highlighted by the recent financial turmoil. But to keep the modeling as simple as possible, counterparty credit risk will here be excluded from further analysis. Models that take account of the presence of counterparty credit risk in the valuation of credit default swaps can be found in for instance Hull & White (2000) or Jarrow & Yu (2001).

2.2 Forward Starting Credit Default Swap

A forward starting CDS is a contract where two parties agree to enter a CDS sometime in the future. The value of such a contract at time t with a CDS starting at time $T > t$, maturing at T_N with payment dates $T_1, T_2, \dots, T_N$ and an annual forward spread S is denoted $V^F(t, T, T_n, S)$ and can be found in a similar fashion to the regular CDS in equation (2.10). Still assuming a notional amount of one, the value of the forwards starting CDS can be expressed as:

$$V^F(t,T,T_N,S) = (1-R)\sum_{m=1}^{M\times(T_N-T)} Z\big(t,\Upsilon_{T,m,M}\big)\big[Q\big(t,\Upsilon_{T,m-1,M}\big)-Q\big(t,\Upsilon_{T,m,M}\big)\big]$$
$$- S\sum_{i=1}^{N}\delta_i\left(Z(t,T_i)Q(t,T_i)+\frac{1}{2}Z(t,\Delta_i)[Q(t,T_{i-1})-Q(t,T_i)]\right) \quad \mathbf{2.13}$$

Let $S^F(t,T,T_N,)$ denote the *forward CDS-premium* at time t, for a CDS starting at T and maturing at time T_N. The forward CDS-premium is the premium of a forward starting CDS ensuring that the contract has a zero value, and can then be written as:

$$S^F(t,T,T_N,) = \frac{(1-R)\sum_{m=1}^{M\times(T_N-T)} Z\big(t,\Upsilon_{T,m,M}\big)\big[Q\big(t,\Upsilon_{T,m-1,M}\big)-Q\big(t,\Upsilon_{T,m,M}\big)\big]}{\sum_{i=1}^{N}\delta_i\left(Z(t,T_i)Q(t,T_i)+\frac{1}{2}Z(t,\Delta_i)[Q(t,T_{i-1})-Q(t,T_i)]\right)} \quad \mathbf{2.14}$$

The forward starting CDS can be valued in a similar manner as the regular CDS in subsection 2.1.4. Since it holds by definition that:

$$V^F\big(t,T,T_N,S^F(t,T,T_N)\big) = 0$$

then

$$V^F(t,T,T_N,S) = V^F(t,T,T_N,S) - V^F\big(t,T,T_N,S^F(t,T,T_N)\big)$$

By inserting equation (2.13) for the respective CDS spreads we can write:

$$V^F(t,T,T_N,S) = \tilde{A}(t,T,T_N)(S^F(t,T,T_N)-S) \quad \mathbf{2.15}$$

where

$$\tilde{A}(t,T,T_N) = \sum_{i=1}^{N}\delta_i\left(Z(t,T_i)Q(t,T_i)+\frac{1}{2}Z(t,\Delta_i)[Q(t,T_{i-1})-Q(t,T_i)]\right)$$

As before, the value of the forward starting CDS depends on the difference between the forward CDS-premium and the premium written in the contract. Also note that at time T, the forward CDS-premium, $S^F(T,T,T_N)$, is equal to the spot CDS premium, where the spot CDS premium is the fair spread of a CDS at time T.

2.3 Credit Default Swaption

A Credit Default Swaption is a contract that gives the holder of the option the right but not the obligation to enter a forward CDS. A credit default swaption does not really fall under the definition of a credit derivative given earlier. It is the underlying, the forward CDS contract, which has a payoff depending on the occurrence of a credit event. However, we will loosen the definition enough to include the credit default swaption in the credit derivatives family. We will consider plain European call options, meaning a contract where the owner has the option to enter a prearranged forward CDS on the protection buyer side at no cost at expiry of the option, often referred to as a *payer swaption*. Should the reference entity underlying the forward CDS default during the life of the option, it will expire worthless. This is referred to as the *knock out feature* (Rutkowski & Armstrong, 2009). The holder of such an option would only enter the forward CDS if the contract has a positive market value at expiry. Let T_E be the expiry date of the option, T be the starting date of the forward CDS and T_N be the maturity of the CDS. Let K be the predetermined spread written in the CDS contract. The value at expiry of the option, $V^{SW}(T_E, T, T_N, K)$, can by the use of the expression for the value of the forward CDS contract in (2.15) be written as:

$$V^{SW}(T_E, T, T_N, K) = 1_{\{\tau > T_E\}} \left(\tilde{A}(T_E, T, T_N)(S^F(T_E, T, T_N) - K) \right)^+ \qquad \textbf{2.16}$$

Where $1_{\{\tau > T_E\}}$ indicates whether or not the reference entity has defaulted before T_E. It is clear from (2.16) that the option will only have a positive value, and hence be exercised, if the forward spread at expiry is larger than the predetermined spread K. Also, from this representation it is clear that the credit default swaption can be seen as an option on the forward CDS spread, with an exercise price equal to the predetermined spread K. This makes the payer swaption easier to understand intuitively. We will return to this representation of the swaption payoff at a later stage.

Now, for simplicity let $T = T_E$, meaning that the option expires on the same day as the forward CDS contract starts. This also means that the forward CDS now is a normal CDS. To reduce the notation somewhat, we write the swaption payoff at expiry as:

$$V^{SW}(T_E, T_E, T_N, K) = 1_{\{\tau > T_E\}} \left(\Pi^{Prot}(T_E, T_N) - \Pi^{Prem}(T_E, T_N, K) \right)^+ \qquad \textbf{2.17}$$

Where $\Pi^{Prot}(T_E, T_N)$ and $\Pi^{Prem}(T_E, T_N, K)$ are given by (2.8) and (2.9) respectively. To find the value at time t of such an option, we return to the principle of risk-neutral valuation introduced in subsection 2.1.1. From equation (2.2), note that we can write the value at time t as:

$$V^{SW}(t, T_E, T_N, K) = Z(t, T_E)\mathbb{E}_t^Q[V^{SW}(T_E, T_E, T_N, K)] \quad \textbf{2.18}$$

Without specifying a model, this is the closest we get to pricing a credit default swaption. Off course, either (2.16) or (2.17) can be inserted for the expression of the swaption value at expiry inside the expectation operator in (2.18). Both representations were presented in this section to differ between the two swaption valuation approaches subsequently introduced in section 5. Before that, section 3 contains a general introduction to credit risk modeling, followed by a more in depth presentation of stochastic intensity models in section 4.

3 Credit Risk Modeling

Broadly speaking there are two approaches to model credit risk, commonly referred to as the *structural approach* and *reduced form approach.* To appreciate the differences of these two, this section will address them both.

3.1 Structural Approach and the Merton Model

The structural approach originates from the theory of option pricing presented by Black & Scholes (1973) and clarified and extended by Merton (1973). With background in this framework, Merton (1974) proposed a model to price risky corporate debt. In the structural approach, explicit assumptions about the dynamics of a firm's asset, its capital structure and its debt are made. In Merton's model the capital structure of the corporation consists of:

- A single homogenous class of debt. The debt can be treated as zero coupon bonds maturing at time T with a total face value of B. Denote the time t value of a defaultable zero coupon bond promising to pay 1 at maturity T as $Z^d(t, T)$. The time t value of the firms debt can then be denoted $Z^d(t, T)B$
- A residual claim, the equity, with time t value E_t.

The firm cannot issue any new claims on the firm nor can it pay dividends to its shareholders. The value of the firm's assets at time t is denoted V_t. By definition, the relationship between the three at any point in time, t, can be written as:

$$V_t = E_t + Z^d(t, T)B \quad \textbf{3.1}$$

The risk-neutral dynamics of the value of the firm's assets are assumed to follow the stochastic differential equation:

$$dV_t = rV_t dt + \sigma V_t dW_t \qquad \textbf{3.2}$$

where r denotes the constant riskless interest rate, σ is the volatility of the assets and W_t is a standard Brownian motion.

The firm promises to pay B to the debt holders at maturity. In the event that the value of the firm's assets are less than the face value of the debt, the bondholders take control of the remaining assets and leave the equity holders with nothing. This means that the time of default, τ, can be expressed as:

$$\tau = \begin{cases} T \ \ if\ V_T < B \\ \infty\ if\ V_T \geq B \end{cases}$$

The risk neutral survival probability from time t to T is equal to the risk neutral probability that the value of the firm's assets is larger than the face value of the bonds at time T:

$$Q(t,T) = Q(V_T \geq B)$$

This expression can easily be solved analytically due to the log-normal specification of the firm's asset value.

The advantages of the Merton-model are its simplicity and intuitive approach, but this also become its disadvantages. The assumption made about the debt of the firm is limiting, as most firms do not have debt consisting of only zero coupon bonds. One should also note that with Merton's setup, default can only happen at maturity. This is both unrealistic as well as it restricts the use of the model. In particular, we are not able to construct a term-structure of survival probabilities, and thus we cannot use this model to price credit derivatives with possible payments at several dates. Attempts to overcome these and other shortcomings have been made, and in the following we will take a quick look at some proposed solutions.

3.1.1 Extensions

Geske (1977) derived a formula to price coupon paying debt by treating the equity of the firm as compound options. On each coupon date before the final payment the equity holders face the option to buy an option maturing on the following coupon date, with an exercise price equal to the coupon payment. The final option to the stockholders is an option on the value of the firm, with an exercise price equal to the face value of the bond plus the last coupon, which is similar to the stockholder option described in Merton's model. The firm issues new equity to finance the coupon payments, which will only be possible as long as the value of the equity is larger than the coupon payment itself. This means that when the equity value is smaller than the coupon payment, the firm will not be able to refinance and it will default. This model can be seen as an improvement over Merton's because it allows the firm to default on different times than the maturity date.

Another approach that allows for default before maturity is the so-called *First-Passage approach* (Black & Cox, 1976). Here, the debt holders have the right to force the firm into default and obtain the remaining of the firm's assets should the firm value fall to a specified level. In effect, the equity holders then have a barrier option on the firm's assets which gets knocked out if the value of the firm touches a barrier. We are then able to find the risk-neutral survival probability up until any point in time as the risk-neutral probability that the value of the firm's assets at that point in time is greater than the barrier. Equipped with these probabilities credit derivatives with multiple possible payments written on the firm can be priced.

Zhou (1997) was one to recognize that a major drawback of models where the firm's assets follow a diffusion process, like equation (3.2), is that firms never default unexpectedly. This is due to the fact that a sudden drop in the firm value under such a process is impossible. To overcome this, Zhou proposed a model where the dynamics of the firm value have two random components. The first is a continuous diffusion component, like in Merton's model, which is meant to characterize the normal changes in the firm's value. The other is a discontinuous jump component that allows for sudden and larger changes in firm value, due to the arrival of new information that impacts the firm value to a larger extent. Zhou argued that this way of modeling the firm value is appropriate when modeling a firm's default risk.

3.2 Reduced Form Approach

Opposed to the structural approach, reduced form models do not connect the event of default to the value of a firm's assets or its debt. Instead, the time of default is seen as a stochastic variable not directly related to any balance sheet information of the firm (Bomfim, 2005, p. 183). The reduced form models lack the intuitive understanding of default supplied by the structural models, but they are popular for their easy implementation and use. In addition, they include the possibility for unexpected default.

Also, as pointed out by Jarrow & Protter (2004), structural models assume complete knowledge of a very detailed information set, information that is not really available to market participants. For instance the asset value process is not observable. The information needed in a reduced form model on the other hand is less detailed, and it can be observed by market participants. Further they believe that when modeling credit risk for pricing and hedging purposes the information needed in a model should be obtainable for market participants, as prices are determined by the market. They therefore argue that the reduced form approach is the right one for pricing and hedging of credit derivatives.

One reduced form approach is to model default as the first arrival of a Poisson process, which is often awarded to the work of Jarrow & Turnbull (1995) and Lando (1998) (See for instance O'Kane, 2008, pp. 45-46). The Poisson process is usually used to model rare events or discretely countable events, and it is reported that the first statistical application of Poisson processes was to model the number of soldiers in the Prussian cavalry that would die due to being kicked by a horse. However, as defaults are rare, and they are discretely countable, the process is also fit for modeling defaults. A Poisson process is defined as (Schönbucher, 2003, p. 113):

A Poisson process N_t *with intensity* $\lambda > 0$ *is a non-decreasing, integer valued process with initial value* $N_0 = 0$ *whose increments are independent and satisfy for all* $0 \leq t < T$*:*

$$Q(N_T - N_t = n) = \frac{1}{n!}(T-t)^n \lambda^n e^{-\lambda(T-t)} \qquad \textbf{3.3}$$

It is this intensity parameter λ which is of our interest, leading to the name of the class of models addressed in this thesis, the intensity models. The next subsections will introduce the framework of the three most common specifications of the intensity of the Poisson process.

3.2.1 Homogeneous Poisson Process

As seen in Jarrow & Turnbull (1995), the simplest specification is to let the intensity be constant, and the jump process is then referred to as a homogeneous Poisson process. As noted above, default is defined as the first jump, meaning that the survival probability between t and T, conditioned on no default before time t, is equal to the probability that the process does not jump in this time period. From equation (3.3) we get:

$$Q(t,T) = Q(N_T - N_t = 0)$$

$$Q(t,T) = \frac{1}{0!}(T-t)^0 \lambda^0 e^{-\lambda(T-t)}$$

$$Q(t,T) = e^{-\lambda(T-t)} \qquad \textbf{3.4}$$

When calibrating the homogenous intensity model to market data, only constant CDS spreads across maturities are possible to obtain. As the term structure of CDS spreads normally is upwards or downwards sloping, it is clear that this model will fail to describe reality. To obtain a more realistic shape of the CDS spread curve, the intensity must be allowed to change through time. By letting the intensity be a function of time, we get an inhomogeneous Poisson process (Schönbucher, 2003, p. 115), to be introduced in the next subsection.

3.2.2 Inhomogeneous Poisson Process

By letting the intensity be a non-negative deterministic function of time, that is, let $\lambda = \lambda_t$, expression (3.3) changes to the following (Schönbucher, 2003, p. 116):

$$Q(N_T - N_t = n) = \frac{1}{n!}\left(\int_t^T \lambda_s ds\right)^n e^{-\int_t^T \lambda_s ds}$$

From this it automatically follows that the survival probability can be expressed as

$$Q(t,T) = e^{-\int_t^T \lambda_s ds}$$

By for instance assuming piecewise constant intensity, this model can be calibrated to market data and replicate the CDS term structure perfectly. However, in a model with deterministic intensities, also the survival probabilities are deterministic. Under the assumption of a constant risk free interest rate and recovery rate, a brief look at expression (2.14) suggests that also the forward CDS spread is deterministic with this specification of the intensity. Clearly, as writing options on anything deterministic is pointless, the deterministic intensity models are not suitable for valuing credit default swaptions. Instead, intensity models allowing the CDS spread to be stochastic should be used when valuing such credit derivatives.

3.2.3 Cox Process

Following Lando (1998) we let the intensity be stochastic. Default is then modeled as the first jump of a *doubly stochastic Poisson process*, also known as a *Cox process*. The intensity is written as $\lambda(X_s)$ where X indicates a stochastic process of state variables and $\lambda(X_s)$ is as before a non-negative function.

Take as given a probability space $(\Omega, \mathcal{F}, Q)$ where $\boldsymbol{Q}$ as before denotes the risk neutral probability measure. Let $\mathcal{G}_t$ denote the filtration generated by the state variables, that is $\mathcal{G}_t = \sigma\{X_s: 0 \leq s \leq t\}$. Further let $\mathcal{H}_t$ hold the information about whether or not a default has happened at time t, meaning $\mathcal{H}_t = \sigma\{N_s: 0 \leq s \leq t\}$, where N_s denotes the jump process. $\mathcal{F}_t$

contains information about both the state variables and whether or not a default has occurred, formally: $\mathcal{F}_t = \mathcal{G}_t \vee \mathcal{H}_t$. The time of default τ is defined as:

$$\tau = inf\left\{t: \int_0^t \lambda(X_s)ds \geq E_1\right\} \qquad \textbf{3.5}$$

where E_1 is a unit exponential random variable independent of the stochastic intensity. This definition of the default time is really no different than before, the only difference is that default is now modeled as the first jump of a Cox process rather than a Poisson process. From (3.5), it becomes obvious that the larger the intensity, the faster the integral grows and higher is the probability that it reaches the level of the unit exponential random variable fast. This implies that the larger the intensity, the higher is the probability of a low τ. The survival probability in the intensity framework can be expressed by:

$$Q(t,T) = 1_{\{\tau>t\}}\mathbb{E}^Q\left(e^{-\int_t^T \lambda(X_s)ds}\middle|\mathcal{G}_t\right) \qquad \textbf{3.6}$$

Note that if we again let the intensity be constant or deterministic we end up with the same expressions for the survival probability as before. Further, expression (3.6) shows that the relationship between the intensity and the survival probabilities is the same as the relationship between a zero coupon bond and the short rate (Duffie & Singleton, 2003, p. 63). By applying suitable term structure models of interest rates to the stochastic intensities, closed form expressions for the survival probabilities exists. Other processes can also be applied to model the intensity, resulting in analytical expressions. In the following section, the intensity models considered in this thesis, which does indeed offer such closed form solutions, will be introduced.

4 Modeling the Intensity

The difference in the three intensity models is the assumed dynamics of the intensity. This section presents the intensity processes, as well as the procedure of simulating them. This will come to use later, when valuing the swaptions. For simplicity we drop the dependence on the state variables in the notation of the stochastic intensity, that is, we write $\lambda(X_s) = \lambda_s$, for the remainder of the thesis.

4.1 CIR Process

A popular choice for modeling the intensity is the CIR process. The process is named after Cox, Ingersoll and Ross (1985) who proposed a single factor model for the term structure of interest rates. Changing the interest rate for the intensity, the dynamics of the intensity λ can in this model be expressed as:

$$\mathrm{d}\lambda_t = \kappa\big(\bar{\lambda} - \lambda_t\big)\mathrm{d}t + \sigma\sqrt{\lambda_t}\mathrm{d}W_t \qquad \textbf{4.1}$$

where $\bar{\lambda}, \kappa, \sigma > 0$. $\bar{\lambda}$ represents the long term value of the intensity. As can be seen from the first term of (4.1), if the intensity at any point is below $\bar{\lambda}$ the drift will be positive and push the intensity towards its long term value. In the opposite case the drift will push the intensity down. The parameter κ determines the speed of the adjustment towards the long term value. σ is the volatility parameter, but as can be seen from the second term of (4.1), the volatility also depends on the level of the intensity. Finally, W_t is a standard Brownian motion.

By imposing the restriction that $2\kappa\bar{\lambda} \geq \sigma^2$, it is secured that the intensity can never reach zero (Feller, 1951), a property required for the Cox-process. To simulate the CIR-process, the approach by Scott (1996, cited in Glasserman, 2003, p.121) is followed. We divide the length of the path we want to simulate into equidistant time steps of length Δt. Let $n = \{1,2, \ldots\}$. The process can then be simulated step by step with the following formula:

$$\lambda_{n\Delta t} = c\big[(\epsilon + \sqrt{L})^2 + X\big] \qquad \textbf{4.2}$$

where

$$\epsilon \sim N(0,1)$$
$$X \sim \chi^2_{d-1}$$
$$d = 4\bar{\lambda}\kappa/\sigma^2$$
$$c = \sigma^2(1 - e^{-\kappa\Delta t})/4\kappa$$
$$L = \lambda_{(n-1)\Delta t}(e^{-\kappa\Delta t})/c$$

This method of simulating the CIR-process relieves us of any discretization errors, and all that is needed is to generate chi-square and standard normal random variables. To generate chi-square random numbers the GKM1 algorithm from Fishman (1996) or Ahrens-Dieter method (Ahrens & Dieter, 1974), depending on the degrees of freedom, is used. For the standard normal variables, the Marsaglia-Bray algorithm is applied. For all, the procedure can be found in Glasserman (2003). Figure 4.1 illustrates a sample path of the CIR-process.

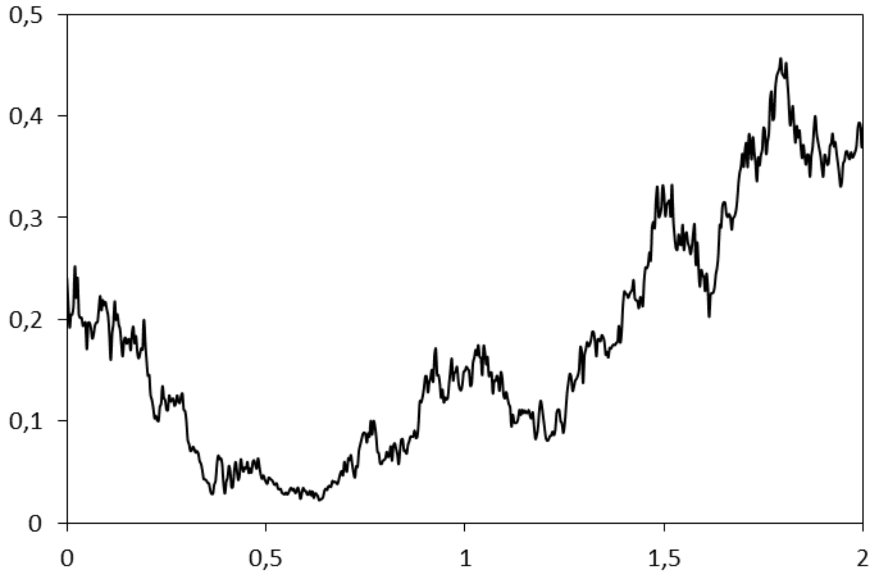

Figure 4.1: *A sample path of the CIR process with parameters* $\boldsymbol{\kappa = 0.65}$, $\boldsymbol{\sigma = 0.22}$, $\boldsymbol{\lambda_o = 0.24}$ *and* $\boldsymbol{\bar{\lambda} = 0.16}$.

By selecting the CIR-process for the intensity, an expression for the survival probability in (3.6) is readily available through the closed form solution derived to value a zero coupon bond, given in Cox et al. (1985):

$$Q(t,T) = 1_{\{\tau>t\}} A(t,T) e^{-B(t,T)\lambda_t} \qquad \mathbf{4.3}$$

where

$$A(t,T) = \left(\frac{2\gamma e^{(\kappa+\gamma)(T-t)\frac{1}{2}}}{(\kappa+\gamma)(e^{\gamma(T-t)}-1)+2\gamma} \right)^{\frac{2\kappa\bar{\lambda}}{\sigma^2}}$$

$$B(t,T) = \frac{2\left(e^{\gamma(T-t)}-1\right)}{(\kappa+\gamma)(e^{\gamma(T-t)}-1)+2\gamma}$$

$$\gamma = \sqrt{\kappa^2 + 2\sigma^2}$$

The analytical expression makes it easy to calibrate the model to observed CDS spreads, and obtain the unknown model parameters; $\kappa, \sigma^2, \lambda_t, \bar{\lambda}$. This enables us to value other credit derivatives, such as the credit default swaption.

4.2 Non-Gaussian Ornstein-Uhlenbeck Processes

Barndorff-Nielsen & Shepard (2001) introduced Non-Gaussian Ornstein-Uhlenbeck processes to describe the changing volatility underlying a financial asset, and they were later used in credit risk modeling by Cariboni & Schoutens (2009) and Kokholm & Nicolato (2010) to model the jump intensity of a Cox-process. The Non-Gaussian Ornstein-Uhlenbeck (OU) process for λ is given by

$$\mathrm{d}\lambda_t = -\theta\lambda_t \mathrm{d}t + \mathrm{dZ}_{\theta t}, \quad \lambda_0 > 0 \qquad \textbf{4.4}$$

where θ is a positive rate parameter and Z a process with independent and stationary increments, a so called Lévy process. This Lévy process drives the OU process, and is therefore referred to as the *background driving Lévy process* (BDLP). As we are looking at Non-Gaussian OU processes, Z is purely jumping, with only positive increments and no drift. This means that the process λ moves up only by jumps and then decreases exponentially. Since $\lambda_0 > 0$, the process is strictly positive. Two different OU processes were employed by Cariboni & Schoutens (2009) to model the jump intensity, the Gamma-OU process and the Inverse Gaussian-OU process. The two processes are obtained by specifying the BDLP so that the intensity is Gamma and Inverse Gaussian distributed respectively and hence the name. The following two sections rely heavily on Cariboni & Schoutens (2009).

4.2.1 Gamma Ornstein-Uhlenbeck Process

To clear out any confusion about the parameterization, it is convenient to state the probability density function of a Gamma distribution with shape parameter a and an inverse scale parameter b. It is given by:

$$f_{Gamma(a,b)}(x) = \frac{b^a}{\Gamma(a)} x^{a-1} e^{-bx} \qquad \textbf{4.5}$$

We will keep this parameterization throughout. The Gamma(a, b)-OU process has a compound Poisson process as a BDLP, given by

$$Z_t = \sum_{j=1}^{N_t} x_j \qquad \textbf{4.6}$$

Where N is a Poisson process with jump intensity a, and x is an independent and identically exponentially distributed variable with rate parameter b. To clarify, x is exponentially distributed with mean $1/b$. This process has a finite number of jumps in every compact time interval.

To simulate the Gamma(a, b)-OU process, we as before divide the length of the path we want to simulate into equal small time steps of length Δt and let $n = \{1,2, ...\}$. The intensity can then be simulated step by step by through the formula:

$$\lambda_{n\Delta t} = e^{-\theta\Delta t}\lambda_{(n-1)\Delta t} + \sum_{j=N_{(n-1)\Delta t}+1}^{N_{n\Delta t}} x_j e^{-u_j\theta\Delta t} \qquad \mathbf{4.7}$$

where N is a Poisson process with intensity parameter $a\theta$, x are as before random exponential distributed variables with rate parameter b, and u are random standard uniform numbers. To simulate the process, we need to first simulate a Poisson process at the time points $n\Delta t$. To do this, note that the jump times of a Poisson process with intensity parameter $a\theta$ is exponentially distributed with a rate parameter $a\theta$ (Bomfim, 2005). We are then able to simulate the Poisson process through simple generation of exponential distributed numbers. The next step is to loop through the Poisson process to find its value at the discrete time points $n\Delta t$. From there on, it is straightforward to simulate the path of a Gamma(a, b)-OU process through (4.7). An example path is presented in Figure 4.2, where the jump nature of the process is apparent. Opposed to the CIR process, which was driven by many small changes in both directions, the Gamma-OU process is steadily declining, only interrupted by positive jumps.

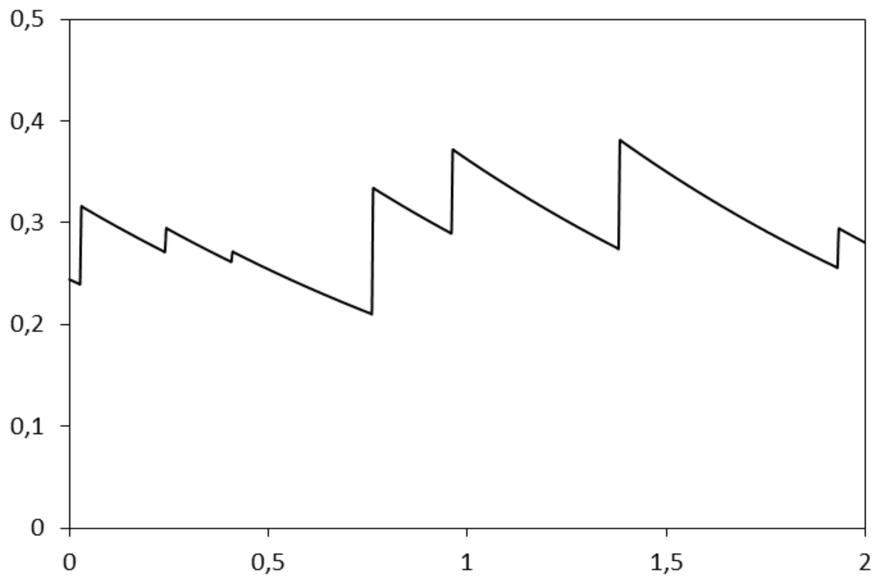

Figure 4.2: *A sample path of the Gamma-OU process, with parameters* $\boldsymbol{\lambda_o = 0.24}$, $\boldsymbol{\theta = 0.73}$, $\boldsymbol{a = 2}$ and $\boldsymbol{b = 13.5}$.

The closed form solution of the right side of (3.6) is given, providing us with the following expression for the risk neutral survival probabilities:

$$Q(t,T) = 1_{\{\tau>t\}}\exp\left(\frac{-\lambda_t}{\theta}\left(1-e^{-\theta(T-t)}\right) - \frac{\theta a}{1+\theta b}\left(b\log\left(\frac{b}{b+\theta^{-1}(1-e^{-\theta(T-t)})}\right)+(T-t)\right)\right) \tag{4.8}$$

Also this expression makes for an easy calibration of the model parameters ; λ_t, θ, a, b, the same amount of parameters as in the CIR-process.

4.2.2 Inverse Gaussian Ornstein-Uhlenbeck Process

The inverse Gaussian distribution with parameters a and b is denoted by IG(a, b), with probability density function:

$$f_{IG(a,b)}(x) = \frac{ae^{ab}}{\sqrt{2\pi}}x^{-\frac{3}{2}}exp\left(-\frac{1}{2}(a^2x^{-1}+b^2x)\right) \tag{4.9}$$

The BDLP of the IG(a, b)-OU process is a sum of two independent Lévy processes, that is:

$$Z_t = Z_t^{(1)} + Z_t^{(2)} \tag{4.10}$$

where $Z_t^{(1)}$ is an Inverse Gaussian Lévy process with parameters $a/2$ and b. $Z_t^{(2)}$ is given by

$$Z_t^{(2)} = b^{-1}\sum_{j=1}^{N_t}\epsilon_j^2 \tag{4.11}$$

N is a Poisson process with jump intensity $ab/2$ and ϵ is an independent and identically distributed standard normal variable. As opposed to the Gamma-OU process, the IG-OU process jumps infinitely often in any time interval.

The algorithm to simulate an IG(a, b)-OU path follows the approach by Zhang & Zhang (2008). We again divide the path into equidistant steps of time Δt, and let $n = \{1,2, ...\}$. The process can be simulated one step of length Δt by the formula:

$$\lambda_{n\Delta t} = e^{-\theta\Delta t}\lambda_{(n-1)\Delta t} + W_0^{\Delta t} + \sum_{j=1}^{\tilde{N}^{\Delta t}} W_j^{\Delta t} \tag{4.12}$$

where

$$W_0^{\Delta t} \sim IG\left(a\left(1-e^{-\frac{1}{2}\theta\Delta t}\right), b\right)$$

$$\tilde{N}^{\Delta t} \sim \text{Poisson}\left(a\left(1-e^{\frac{1}{2}\theta\Delta t}\right)b\right)$$

and $W_j^{\Delta t}$, for $j = \{1,2 \dots . \tilde{N}^{\Delta t}\}$ are independent and identically distributed random variates from the density $f_{W^{\Delta t}}(x)$, where

$$f_{W^{\Delta t}}(x) = \begin{cases} \dfrac{b^{-1}}{\sqrt{2\pi}} x^{-\frac{3}{2}}\left(e^{\frac{1}{2}\theta\Delta t}-1\right)^{-1}\left(e^{-\frac{1}{2}b^2x}-e^{-\frac{1}{2}b^2xe^{\theta\Delta t}}\right), & x > 0 \\ 0 & otherwise \end{cases} \qquad \textbf{4.13}$$

The following algorithm generates $W_j^{\Delta t}$.

- **Step 1**: Generate $Y \sim Gamma\left(\frac{1}{2}, \frac{1}{2}b^2\right)$
- **Step 2**: Generate $U \sim Uniform(0,1)$
- **Step 3**: Set $g(Y) = \frac{\sqrt{\frac{1}{2}b^2}}{\Gamma\left(\frac{1}{2}\right)} Y^{-\frac{1}{2}} e^{-\frac{1}{2}b^2 Y}$
- **Step 4**: If $U \leq \frac{f_{W^{\Delta t}}(Y)}{\frac{1}{2}\left(1+e^{\frac{1}{2}\theta\Delta t}\right)g(Y)}$ then $W_j^{\Delta t} = Y$. Otherwise, return to step 1. $f_{W^{\Delta t}}(Y)$ is given in (4.13)

Inverse Gaussian random numbers are generated through the algorithm based on Michael et al. (1976), the Poisson variate through the inverse transform method and the Gamma(a, b) random numbers through the GKM1 algorithm from Fishman (1996) or Ahrens-Dieter method (Ahrens & Dieter, 1974) depending on the value of a. As before, all these procedures are found in Glasserman (2003).

The IG(a, b)-OU path can be simulated by applying (4.12) recursively. A sample path is depicted in Figure 4.3. A comparison with the Gamma-OU process indicates that the IG-OU process is driven by more jumps, but of lower jump size.

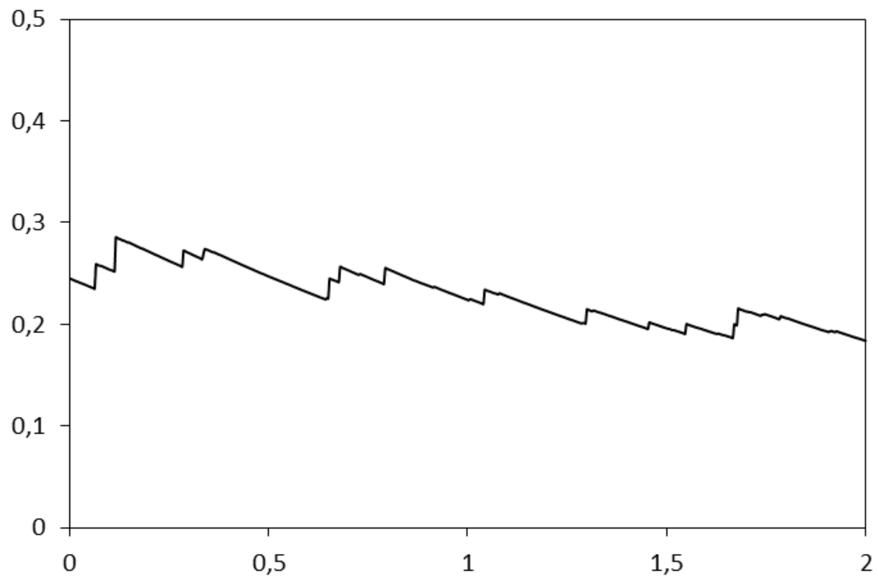

Figure 4.3: *A sample path for the IG-OU process. Parameters are* $\boldsymbol{\lambda_o = 0.25}$, $\boldsymbol{\theta = 0.69}$, $\boldsymbol{a = 1.29}$ and $\boldsymbol{b = 9.34}$.

The risk neutral survival probabilities are found through the Laplace transform, and can be expressed as:

$$Q(t,T) = 1_{\{\tau>t\}} exp\left(\frac{-\lambda_t}{\theta}\left(1-e^{-\theta(T-t)}\right) - \frac{2a}{b\theta}B(t,T)\right) \qquad \textbf{4.14}$$

Where

$$B(t,T) = \frac{1-\sqrt{1+v(1-e^{-\theta(T-t)})}}{v} + \frac{1}{\sqrt{1+v}}\left[arctanh\left(\frac{\sqrt{1+v(1-e^{-\theta(T-t)})}}{\sqrt{1+v}}\right) - arctanh\left(\frac{1}{\sqrt{1+v}}\right)\right]$$

$$v = \frac{2}{\theta b^2}$$

The derivation can be found in Nicolato & Venardos (2003). Also in the case of the IG-OU process, there are four parameters that needs to be calibrated; λ_t, θ, a, b.

5 Valuing Credit Default Swaptions

While the two previous sections were focusing on how to model the default of an entity, the following section will more specifically address how credit default swaptions can be valued. In the first subsection the intensity model framework will be temporary abandoned to introduce the market model, which allows for a simple expression of the swaption value. In the subsequent subsection the intensity framework will again be assumed, focusing on how to value credit default swaptions with a stochastic intensity model.

5.1 The Market Model

Several papers have addressed the issue of valuing credit default swaptions, among them Jamshidian (2004), Schönbucher (2004) and Brigo (2005). Under different assumptions, they used the *change of numéraire technique* to develop a pricing formula for swaptions. A general description follows, inspired by O'Kane (2008). First, return to the expression for the value of the swaptions at maturity given in (2.16), rewritten here:

$$V^{SW}(T_E, T_E, T_N, K) = 1_{\{\tau > T_E\}} \tilde{A}(T_E, T_E, T_N)(S^F(T_E, T_E, T_N) - K)^+ \qquad \textbf{5.1}$$

Note that the initiation of the underlying CDS contract is for simplicity set equal to the expiry date of the swaption, that is $T = T_E$. In subsection 2.1.1 it was argued that the price of an asset is equal to the expected value of the asset under the risk neutral measure, discounted with the risk free rate. In that case $S_t = e^{\int_0^t r(s)ds}$ was the numéraire, and belonging to it was the risk neutral probability measure $\boldsymbol{Q}$**,** under which the price process relative to the numéraire was a martingale. In general, for any numéraire there is a probability measure under which the relative price process is a martingale. Now, let X_t be a price process and let A_t be a numéraire. Then, under the assumption of no arbitrage there is a probability measure, denoted $\boldsymbol{A}$**,** under which the relative price process is a martingale. This means that:

$$\frac{X_t}{A_t} = \mathbb{E}_t^A \left[\frac{X_T}{A_T}\right] \qquad \textbf{5.2}$$

We refer to the probability measure $\boldsymbol{A}$ as the *annuity measure*, and $\mathbb{E}_t^A[\cdot]$ denotes the expectation taken under this measure. A possible choice of numéraire is to set $A_t = 1_{\{\tau > t\}} \tilde{A}(t, T_E, T_N)$. If we let X_t be the price process of the swaption, the value of the swaptions at time t can then by (5.1) and (5.2) be written as:

$$V^{SW}(t, T_E, T_N, K) = 1_{\{\tau > t\}} \tilde{A}(t, T_E, T_N) \mathbb{E}_t^A[(S^F(T_E, T_E, T_N) - K)^+] \qquad \textbf{5.3}$$

To choose $A_t = 1_{\{\tau > t\}} \tilde{A}(t, T_E, T_N)$ is a bit problematic, since it is not really a valid numéraire. As pointed out by for instance Jamshidian (2004), it fails to satisfy an important condition of a numéraire; to be a strictly positive process. Should the reference entity default at a time before t, we will have $A_t = 0$, and the condition would be violated. However, due to the knockout feature, we know that if $A_t = 0$ then the swaption payoff is also zero. This is used as an argument to make an exception and indeed let the numéraire be $A_t = 1_{\{\tau>t\}}\tilde{A}(t, T_E, T_N)$.

From (5.3), it is easy to see that a credit default swaption can be thought of as a call option on the forward CDS spread, with a strike K, as argued before. The next step in deriving what Brigo (2005) calls a *market formula* for swaptions is to make an assumption on the dynamics of the forward CDS rate. The common approach is to assume that the forward CDS spread follows a geometric Brownian motion under the annuity measure, with no drift. That is, the forward spread follows:

$$dS^F(t, T_E, T_N) = \sigma S^F(t, T_E, T_N) dW_t^A$$

This implies that the forward spread is lognormal with volatility parameter σ. This assumption is popular, as the value of a credit default swaption then can be found through the so called Black (1976) formula:

$$V_{Black}^{SW}(t, T_E, T_N, K, S^F, \sigma) = \tilde{A}(t, T_E, T_N)[S^F(t, T_E, T_N)\Phi(d_1) - K\Phi(d_2)] \qquad \textbf{5.4}$$

Where

$$d_1 = \frac{\ln\left(\frac{S^F(t, T_E, T_N)}{K}\right) + \frac{1}{2}\sigma^2(T_E - t)}{\sigma\sqrt{T_E - t}}$$

$$d_2 = d_1 - \sigma\sqrt{T_E - t}$$

The simplicity of the model is appealing, as we only need one unobservable input parameter to calculate an option price, the constant volatility parameter σ. However, Brigo & El-Bachir (2006) suggest that the model is a rather primitive approximation, which perhaps is better used for quoting swaptions in terms of the volatility implied by the model formula. Instead they propose to price credit default swaptions with the use of stochastic intensity models.

5.2 Credit Default Swaptions in an Intensity Model

Hedging and valuation of default swaptions in the CIR-intensity model were discussed in Bielecki et al. (2011), and in an extended version of the CIR-process where shifts and jumps were included, a semi-analytical formula for pricing swaptions was derived (Brigo & El-Bachir, 2007). This formula was built on a formula for swaptions under the lesser extension allowing only for shifts by Brigo & Alfonsi (2005). We are dealing with somewhat different models and will resort to other techniques to value credit default swaptions.

Now, return to the set up in section 3.2.3. That is, take as given a probability space $(\Omega, \mathcal{F}, Q)$. $\mathcal{F}_t$ denotes the full filtration, and $\mathcal{F}_t = \mathcal{G}_t \vee \mathcal{H}_t$, where, $\mathcal{G}_t$ holds the information about the intensity and $\mathcal{H}_t$ contains information on whether or not a default has occurred. In section 2.3 it was argued that the time t value of a payer credit default swaption could be expressed as:

$$V^{SW}(t, T_E, T_N, K) = Z(t, T_E)\mathbb{E}_t^Q\left[1_{\{\tau > T_E\}}\left(\Pi^{Prot}(T_E, T_N) - \Pi^{Prem}(T_E, T_N, K)\right)^+\right] \qquad \textbf{5.5}$$

where as before

$$\Pi^{Prot}(T_E, T_N) = (1 - R) \sum_{m=1}^{M\times(T_N - T_E)} Z\left(T_E, \Upsilon_{T_E,m,M}\right)\left[Q\left(T_E, \Upsilon_{T_E,m-1,M}\right) - Q\left(T_E, \Upsilon_{T_E,m,M}\right)\right]$$

$$\Pi^{Prem}(T_E, T_N, K) = K \sum_{i=1}^{N} \delta_i \left(Z(T_E, T_i)Q(T_E, T_i) + \frac{1}{2}Z(T_E, \Delta_i)[Q(T_E, T_{i-1}) - Q(T_E, T_i)]\right)$$

and T_E is the expiry date of the swaption. The CDS contract is initiated at the expiry of the swaption and matures at T_N with payment dates $T_i > T_E$ for $i = \{1,2 \ldots . N\}$. K is the predetermined annual spread. Recall that the closed form solution for the survival probability between T_E and T_i for the three intensity models was conditioned on the survival up until time T_E. Through the knockout feature, this has been accounted for, ensuring that the closed form solutions are applicable when calculating the protection- and premium leg.

Further assume that the well-known relation for a random variable Y holds (see for instance Jeanblanc & Rutkowski, 2002):

$$\mathbb{E}^Q\left[1_{\{\tau > T\}}Y|\mathcal{F}_t\right] = 1_{\{\tau > t\}}\mathbb{E}^Q\left[e^{-\int_t^T \lambda_s ds}Y|\mathcal{G}_t\right] \qquad \textbf{5.6}$$

Recall that $\mathbb{E}_t^Q[\cdot]$ denotes the expectation under the risk neutral probability measure, based on all information at time t. That is; $\mathbb{E}_t^Q[\cdot] = \mathbb{E}^Q[\cdot\,|\mathcal{F}_t]$. Through (5.6), expression (5.5) can then be written as:

$$V^{SW}(t, T_E, T_N, K) = 1_{\{\tau > t\}}Z(t, T_E)\mathbb{E}^Q\left[e^{-\int_t^{T_E} \lambda_s ds}\left(\Pi^{Prot}(T_E, T_N) - \Pi^{Prem}(T_E, T_N, K)\right)^+|\mathcal{G}_t\right] \qquad \textbf{5.7}$$

This is convenient, because swaptions can be valued conditioned only on the filtration generated by the stochastic intensity process. The advantages of this will be apparent shortly. Solving the expectation in (5.7) analytically is not trivial, however. Therefore, we will resort to numerical methods, namely the Monte Carlo Method.

5.2.1 Monte Carlo Method

The following introduction to the Monte Carlo Method is inspired by Schönbucher (2003, p. 212) and Glasserman (2003, pp. 2-6). Let $X(\omega)$ be a random variable, and suppose the valuation problem can be represented as:

$$C = \mathbb{E}[X(\omega)]$$

where C may very well be the price of some credit derivative. The solution of the expectation can be found by generating a large number P of independent samples $x_p = X(\omega_p)$ for $p = \{1,2 \dots . P\}$. An unbiased estimator that approximates the "true" value of C is then:

$$\hat{C} = \frac{1}{P}\sum_{p=1}^{P} x_p$$

The intuition behind the method is quite clear. To solve the expectation, a large number of possible outcomes is generated, where each possible outcome is assigned with an equal probability. The *law of large numbers* ensures that as P goes towards infinity, the estimator goes towards the true value. Formally:

$$\hat{C} \to C \quad as \quad P \to \infty$$

The error in the Monte Carlo estimate can also be measured. The difference between the estimator and the "true" value, $\hat{C} - C$, is approximately normally distributed with mean zero and a standard deviation of $\sigma_X/\sqrt{P}$, where σ_X denotes the standard deviation of $X(\omega)$. Generally σ_X is not known, but it can be estimated through the sample standard deviation:

$$s_X = \sqrt{\frac{1}{P-1}\sum_{p=1}^{P}\left(X(\omega_p) - \hat{C}\right)^2}$$

A confidence interval for the price can then be formed. Let z_δ denote the $(1-\delta)$ quantile of the standard normal distribution. A $(1-\delta)$ confidence interval for the price can then be approximated by

$$\hat{C} \pm z_{\delta/2}\frac{s_X}{\sqrt{P}}$$

As can be seen, the quality of the estimator can be improved by increasing the number of generated samples. Naturally, the computational cost will then increase, and there will be a tradeoff between accuracy and precision. As the precision will be of high importance in valuation problems, the Monte Carlo method can sometimes be a slow pricing method.

5.2.2 Valuing Swaptions with Monte Carlo Simulation

Let us return to the specific valuation problem in equation (5.7). Since we have assumed a fixed risk free interest rate and recovery rate, a sample of the swaption value at maturity can be generated given the model parameters. More specifically, given the four model parameters in one of the intensity models introduced in this thesis, a sample of the intensity's path from t to T_E is all that is needed to obtain a sample of the swaption value. On the basis of this path, the quantity $\exp(-\int_t^{T_E} \lambda_s ds)$ can be calculated, and the survival probabilities in the protection and premium leg can be calculated when we have a sample of λ_{T_E}. By generating a large number of swaption values, an unbiased estimator can then be obtained by simply calculating the discounted average of all sample values. Now the attraction of the switch from $\mathcal{F}_t$ to $\mathcal{G}_t$ is apparent. Due to this switch, no attention needs to be directed to whether or not the Cox process jumps. Instead, only the intensity process is of interest. Clearly, this eases the generation of swaption value samples. This approach to valuing swaptions is equivalent to the one taken by Brigo & El-Bachir (2006).

The stepwise procedure used to implement the pricing method is listed below:

- **Step 1**: Divide the interval $[t, T_E]$ into $\#N$ equidistant time steps of length Δt.
- **Step 2:** For a given parameter set, simulate a path of the intensity from t to T_E at the fixed time points $n\Delta t$ where $n = \{1,2..\#N\}$
- **Step 3:** Calculate a sample value for a given strike K by the formula:

$$x_p = Z(t, T_E)\exp(-\int_t^{T_E} \lambda_s ds)\left(\Pi^{Prot}(T_E, T_N) - \Pi^{Prem}(T_E, T_N, K)\right)^+$$

  where $\exp(-\int_t^{T_E} \lambda_s ds)$ is approximated by $\exp\left(-\sum_{n=1}^{\#N} \lambda_{(n-1)\Delta t}\Delta t\right)$.
- **Step 4:** Repeat step 3 a large number P times.
- **Step 5:** Calculate the swaption value by:

$$\hat{V}^{SW}(t, T_E, T_N, K) = \frac{1}{P}\sum_{p=1}^{P} x_p$$

This concludes the section about how to value credit default swaptions. Next section will introduce the methodology used to perform the analysis of how suitable the intensity models are for valuing credit default swaptions when they are calibrated to market prices of credit default swaps.

6 Methodology

The performance of the three intensity models will be analyzed through a threefold investigation. This section introduces the approach to the three aspects, calibration, swaption valuation and implied volatilities.

6.1 Calibration

As the closed form solutions for the survival probabilities for the three intensity models are given by (4.3), (4.8) and (4.14), the models can be directly calibrated to credit default swap market quotes by minimizing the Sum of Squared Errors (SSE):

$$SSE = \sum_{q=1}^{8} \left(S_q^{Market} - S_q^{Model} \right)^2 \qquad \textbf{6.1}$$

where S^{Market} denotes the spread observed in the market, and S^{Model} is the model spread as expressed in (2.11). The minimizing procedure is performed using the Solver in MS Excel.

6.1.1 Market Data

The obtained market quotes are displayed in Table 6.1. As can be seen, the perceived credit quality of the three reference entities ranges from very high (Nestlé) to very poor (National Bank of Greece). In between there is Royal Bank of Scotland. The idea behind choosing these reference entities is to investigate whether or not the perceived credit quality has any influence on the performance of the intensity models.

Maturity	**Nestlé**	**Royal Bank of Scotland (RBS)**	**National Bank of Greece (NBG)**
0.5	6.56	58.45	1343.32
1	7.55	66.33	1357.70
2	12.20	97.44	1190.12
3	17.38	133.64	1096.76
4	24.91	165.56	1072.99
5	32.43	197.26	1059.80
7	44.24	224.30	1013.01
10	54.93	238.59	984.84

Table 6.1: *CDS market spreads for different maturities. Obtained on March 19th, 2013.*

The spreads are quoted on March 19th. The choice of date is no coincidence, but rather a result of what is referred to as the *quarterly roll*. Since 2003, the convention for determining the maturity date of a standard CDS contract has been changed. Before this, most contracts had a maturity of *T*-years from the initiation of the contract. This meant that a market participant that wished to hedge a recently transacted CDS contract would face a credit exposure in the future, unless the hedge was carried out on the exact same day as the original trade. The only way to avoid this was to enter a non-standard contract with the same maturity date as the original trade, but generally a non-standard contract is more costly as they are less liquid. This issue was addressed by starting to trade contracts maturing at standard maturity dates. The dates chosen were March 20th, June 20th, September 20th and December 20th. This means that after 2003, the standard contract with a maturity of T-years had a maturity date on the first of the standard dates after T-years (O'Kane, 2008, p. 83). Figure 6.1 illustrates how the maturity date is linked to the trade date.

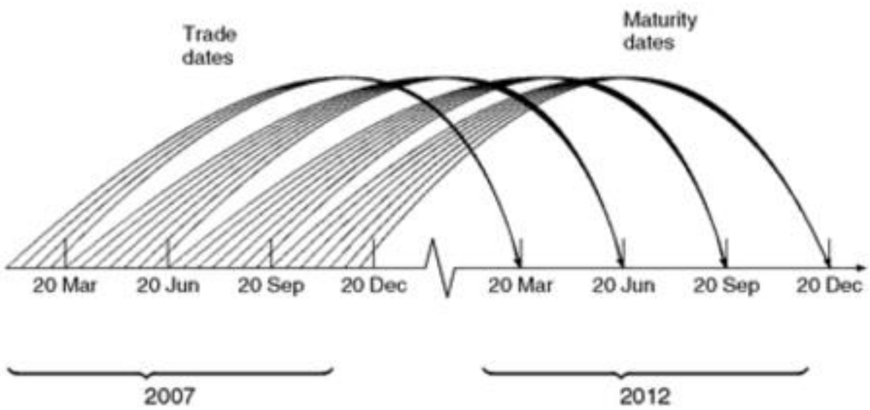

Figure 6.1: The quarterly roll. Example of CDS with five-year length. The maturity of the contract is the first standard date five years after trade date. *Source: O'Kane (2008, p. 83)*

The result of this is that a standard T-year CDS contract has maturity of T-years to T-years plus three months, depending on when the contract is entered. By using market data from one day before a standard date, it is ensured that the T-year CDS contracts in the dataset really are as close as possible to maturing after T-years. Then we can set $t = T_0 = 0$, without any large errors. Ignoring that some payments will fall on weekends or holidays, this eases calculations of the model spread since the distance between a payment date and the next will be equal for all payment dates, that is $\delta_i = \delta$ for all $i = \{1,2 \dots N\}$. Further, assuming that the market standard holds, so that premium payments are paid quarterly, we have $\delta = 0.25$. This also means that for a contract maturing in y years, $N = y \cdot 4$.

Finally, following Houweling & Vorst (2005), the discrete grid of time points where default can happen is set at a monthly interval, i.e. $M = 12$.

6.1.2 Choice of Risk Free Rate and Recovery Rate

The choice of risk free rate will not have much effect on the model spread, since both the protection leg and premium leg are discounted with the same rate. Based on the current low interest rate environment, the risk free rate is fixed at 2 %.

Both Elizalde (2005) and Houweling & Vorst (2005) valued credit default swaps with deterministic intensity models, and both found that as long as the recovery rate is in a reasonable interval, credit default swap spreads are relatively insensitive to different assumed recovery rates. A reasonable interval is argued to be between 20 % and 60 %. In applications of stochastic intensity models, recovery rates are usually fixed between 30 % and 40 % (See for instance Brigo & El-Bachir (2007) and Cariboni & Schoutens (2009)). Based on this, a fixed recovery rate of 40 % seems reasonable.

6.1.3 Different Intervals

In the investigation of how different the parameter sets obtained can be and how these different sets affect swaption values, the first step is to initialize the calibration procedure with different starting values. This is done by choosing an interval for each parameter we want to calibrate, and then automatically loop through different combinations of starting values in these intervals, each time starting the minimizing procedure. For all calibrations, no limits for maximum time or number of iterations are set. For every entity three parameter sets from each model will be selected and investigated further. As a measure of the quality of fit between the market and the model spreads obtained with these parameters, the *average relative percentage error* (ARPE) is also calculated.

$$ARPE = \frac{1}{8}\sum_{q=1}^{8} \frac{\left|S_q^{Market} - S_q^{Model}\right|}{S_q^{Market}} \qquad \textbf{6.2}$$

Since the ARPE is a difference measure relative to the marked CDS spread, the ARPE from calibration on high credit quality reference entities are often higher due to the low CDS spread.

6.1.3.1 Calibrating the CIR model

Based on trial and error, an interval has been selected for each unknown parameter, listed in Table 6.2. Within this interval a procedure has been started, which uses a total of 1296 parameter combinations as starting values for each entity, resulting in a large number of proposed solutions.

	$\boldsymbol{\kappa}$	$\boldsymbol{\sigma^2}$	$\boldsymbol{\lambda_0}$	$\boldsymbol{\bar{\lambda}}$
Nestlé	0.001-1.501	0.0001-0.5001	0.00001-0.00101	0.01-0.76
RBS	0.01-1.51	0.01-0.76	0.0001-0.0151	0.01-1.01
NBG	0.01-1.51	0.01-0.76	0.01-0.76	0.01-1.01

Table 6.2: The intervals for the different starting values of each parameter.

Motivated by the effect volatility has on option values, for the CIR model, the main focus was to select solutions with different volatility parameters. All else equal, a high volatility will increase the probability of a high intensity. A high volatility parameter should then lead to a higher value of the swaption, since the CDS spread is an increasing function of the intensity. However, normally all is not equal, so it will be interesting to see how the other parameters are able to cancel out the effect of differences in the volatility parameter.

6.1.3.2 Calibrating the Gamma Ornstein-Uhlenbeck model

For the Gamma-OU process we searched for solutions with starting values for the parameters in the intervals listed in Table 6.3. Once again, the intervals have been adapted after a trial and error exercise and these intervals are meant to cover the parameter values which are able to provide a good fit of the model.

	$\boldsymbol{\lambda_0}$	$\boldsymbol{\theta}$	$\boldsymbol{a}$	$\boldsymbol{b}$
Nestlé	0.00001-0.00151	0.01-2.01	0.01-15.01	0.01-100
RBS	0.0001-0.0151	0.01-2.01	0.01-50.01	0.01-1000
NBG	0.01-0.76	0.01-1.61	0.01-5.010	0.01-20.01

Table 6.3: The intervals for the different starting values of each parameter.

Note that the interval for a and b are quite wide. This is because it seems as if a high value of a can be compensated by a high value of b. A possible explanation for this can be found by recalling that the BDLP of the Gamma-OU process was a compound Poisson process, where a is the jump intensity of the Poisson process. So a high a causes the Poisson process to jump more often. However, the jump size of the process has a mean of $1/b$. This means that the increased number of jumps can be compensated by a lower jump size, that is, a higher b.

6.1.3.3 Calibrating the Inverse Gaussian Ornstein-Uhlenbeck model

Table 6.4 shows the intervals where we searched for solutions for the IG-OU process.

	$\boldsymbol{\lambda_0}$	$\boldsymbol{\theta}$	$\boldsymbol{a}$	$\boldsymbol{b}$
Nestlé	0.00001-0.00151	0.001-2.01	0.01-5.01	0.01-40.01
RBS	0.0001-0.0151	0.001-2.01	0.01-7.51	0.01-100.01
NBG	0.01-0.76	0.01-2.01	0.01-2.51	0.01-10.01

Table 6.4: *Intervals of different starting values in the calibration of IG-OU process.*

Also here the intervals for a and b are quite wide, as parameter sets with quite big differences in these parameters are observed. Again, a possible explanation for this phenomenon can be found by recalling the BDLP of the IG-OU process. The IG-Lévy process which is the first of the two independent Lévy processes driving the BDLP has a mean of $0.5 \cdot a/b$, where it is clear how the two parameters can compensate an increase in each other's values. The other Lévy process was defined as, from equation (4.11):

$$Z_t^{(2)} = b^{-1} \sum_{j=1}^{N_t} \epsilon_j^2$$

Where $N \sim Poisson(ab/2)$ and $\epsilon \sim N(0,1)$. Higher values of a and b will thus increase the number jumps, but the constant b^{-1} will reduce the effect of these jumps.

For both the Gamma- and the IG-OU model, the focus has been on selecting parameter sets with different values of a and b, to investigate the effects in swaption valuation.

6.2 Credit Default Swaption Valuation

In the application of the valuation procedure described in section 5, we concentrate on swaptions maturing in one year, with an underlying CDS contract with a length of five years. That is; $t = 0$, $T_E = T_0 = 1$ and $T_N = 6$. The length of the path is divided into 300 equidistant time steps and the estimated swaption values are calculated based on 40 000 sample paths.

To properly compare the swaption prices within and across models, swaption prices for different predetermined CDS spreads K need to be calculated. Recall that the swaption can be seen as a call option on the forward CDS spread, with a strike equal to K. It therefore makes sense to select the different strikes based around the current forward spread. For each of the three reference entities, swaption prices for ten different strikes are calculated. This does not affect the computational time in any particular way, as swaption sample values for all ten strikes are calculated after each single path.

The *relative difference* between the swaption values from two parameter sets, i, j, for a given strike is calculated by:

$$Relative\ Difference = \frac{\left|V_{(i)}^{SW}(K) - V_{(j)}^{SW}(K)\right|}{Min\left(V_{(i)}^{SW}(K); V_{(j)}^{SW}(K)\right)} \qquad \textbf{6.3}$$

The relative difference is meant to serve as a measure of the mispricing caused by the different parameter sets. The relative difference tends to be higher for lower swaption prices, not unlike what was argued for the ARPE above. Direct comparison should therefore be done with caution, but in any case, a relative difference will give guidance to the severity of the mispricing between two parameter sets.

6.3 Implied Volatility Smiles

An interesting part of the analysis is to investigate the *implied volatility smiles* generated by the different models and parameter sets. As pointed out in Brigo & El-Bachir (2006), the constant volatility parameter in the Black formula does not describe reality satisfactory. Instead one would in the market expect to observe different volatility parameters for different strikes, and thus a so called volatility smile, or more correctly a smirk, would be present. Any model that aims to price swaptions consistently should therefore be able to generate a realistic smile of implied volatilities.

The term implied volatility alludes to the value of the volatility parameter, from now on denoted σ^{im}, which for a given swaption price, forward spread, strike and maturity solves the equation:

$$V^{SW}(t, T_E, T_N, K) = V_{Black}^{SW}\left(t, T_E, T_N, K, S^F, \sigma^{im}\right)$$

Implied volatility analysis for swaption prices calculated under the shifted square root diffusion (SSRD) intensity model can be found in Brigo & Cousot (2006). A volatility smile analysis for the jump extended SSRD model is performed by Brigo & El-Bachir (2006). In Jönsson & Schoutens (2007) the presence of a realistic implied volatility smile generated by a default model where the *firm value* follows a Shifted Gamma model, a model where the firm value has a positive drift with negative jumps coming from a Gamma(a, b) process, is argued to be an important feature of the model.

Due to the scarcity of data on credit default swaptions, what constitutes as a realistic volatility smile has to be inferred from the previously mentioned analyses of implied volatility smile. In those it seems as if a smile increasing with the strike is most plausible.

6.3.1 Newton-Rhapson Method

The implied volatilities are found using the Newton-Rhapson Method. For an initial guess of the implied volatility, σ_o^{im}, this guess can be improved by the formula:

$$\sigma_1^{im} = \sigma_o^{im} - \frac{\left(V_{Black}^{SW}\left(\sigma_0^{im}\right) - V^{SW}\right)}{\frac{\partial V_{Black}^{SW}\left(\sigma_0^{im}\right)}{\partial \sigma^{im}}}$$

where the notation of the observed parameters t, T_E, T_N, K, S^F has been dropped. An iteration procedure by the general formula in (6.4) will improve the estimate and in most cases converge to the true implied volatility after few iterations. (See for instance Kritzman(1991)).

$$\sigma_{n+1}^{im} = \sigma_n^{im} - \frac{\left(V_{Black}^{SW}\left(\sigma_n^{im}\right) - V^{SW}\right)}{\frac{\partial V_{Black}^{SW}\left(\sigma_n^{im}\right)}{\partial \sigma^{im}}} \qquad \textbf{6.4}$$

In the implementation of the Newton-Rhapson Method, 100 iterations are performed, which should be satisfactory in all cases where the true implied volatility can be found. Unfortunately, as the data set does not contain observed forward spreads, they need to be estimated. As the models are inclined to produce slightly different estimates, the forward price is fixed based on the indications of the different model estimates when extracting the implied volatility. The annuity also needs to be calculated by the different models through the survival probabilities. However, in this case, there does not seem to be any differences, ensuring that different implied volatilities between the models are caused due to a difference in the estimated swaption values.

7 Results

In this section the empirical results are presented and analyzed. For each reference entity, three different parameter sets obtained in the calibration are selected from each of the three models. The first parameter set from each model is the parameter set that yields the lowest sum of squared errors, and the two others are selected on the basis of interesting differences in parameter values while at the same time being similar to the first parameter set in terms of ARPE or SSE. The corresponding credit default swaption prices obtained by each of these three parameter sets will be shown graphically. The swaption values are quoted in basis points, to avoid having to deal with very small numbers. Further, the implied volatility smiles generated by the different swaption values from the parameter sets are presented. The results for each reference entity are concluded with a comparison of the models. Here we present the minimum, maximum and average relative difference across the strike values for all combinations of parameter sets for each model, before we compare and highlight the difference in the values and implied volatilities generated by the models.

The appendix contains the swaption values along with their 95 % confidence error and implied volatilities in table form. The appendix also contains an explanation to the data appendix which consists of three MS Excel files, one for each reference entity, where the spreadsheets and VBA code implementing the analysis can be found.

7.1 Nestlé

For Nestle, the forward CDS spread calculated by the models is seemingly around 43 basis points. Based on this, the forward spread is fixed at 43 bp, and ten swaption prices with strikes in the interval $[25-70]$ with steps of 5 basis points are calculated for the selected parameter sets from each model.

7.1.1 CIR Intensity

The three chosen parameter sets for Nestlé are presented in Table 7.1 along with their corresponding average relative percentage error and sum of squared errors.

	$\boldsymbol{\kappa}$	$\boldsymbol{\sigma^2}$	$\boldsymbol{\lambda_0}$	$\boldsymbol{\bar{\lambda}}$	**ARPE**	**SSE**
Set 1	0.017	0.00419	0.00024	0.1203	9 %	21.84
Set 2	0.035	0.00009	0.00022	0.0622	9.2 %	22.65
Set 3	0.017	0.00084	0.00030	0.1197	8.9 %	22.86

Table 7.1: *Parameter sets selected for Nestlé from the calibration of the CIR process.*

Generally, it is clear that all three sets reflect Nestlé's low default risk with a fairly small λ_0. Another general observation, looking at the long term mean, is that the intensity is bound to increase. The three parameter sets are comparable in terms of their fit to the market spreads and the sum of squared errors. Set 1 and 3 are actually quite similar in every aspect, except from in their volatility, where the squared volatility of set 1 is almost five times higher. Set 2 has the lowest volatility, but also a higher speed reversion and a lower long term mean than the other two parameter sets.

Theoretical credit default swaption values for the three parameter sets are presented in Figure 7.1.

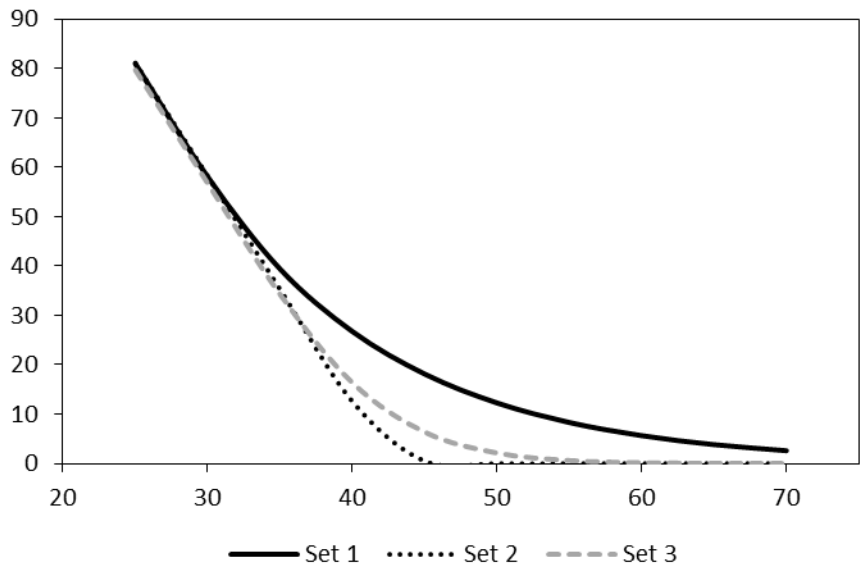

Figure 7.1: *Swaption prices as a function of the strike for Nestlé, generated by three different parameter sets from the CIR model. The forward spread is 43 bp.*

For low strikes, the three parameter sets seem to give quite similar swaption values. However, as the strike increases, a higher volatility leads to a higher swaption value for a given strike. This volatility effect was expected for the CIR model. Most dramatic are the results for parameter set 2. Here, the swaption values are very low for strikes of 45 and 50 bp, and equal to zero for a strike of 55 bp and upwards. Due to the low volatility, combined with a low long term mean, the intensity is never able to move to a level where the spot CDS spread at expiry is larger than 55 basis points, and only very few cases where it is larger than 45. The corresponding implied volatilities for the theoretical prices are in Figure 7.2.

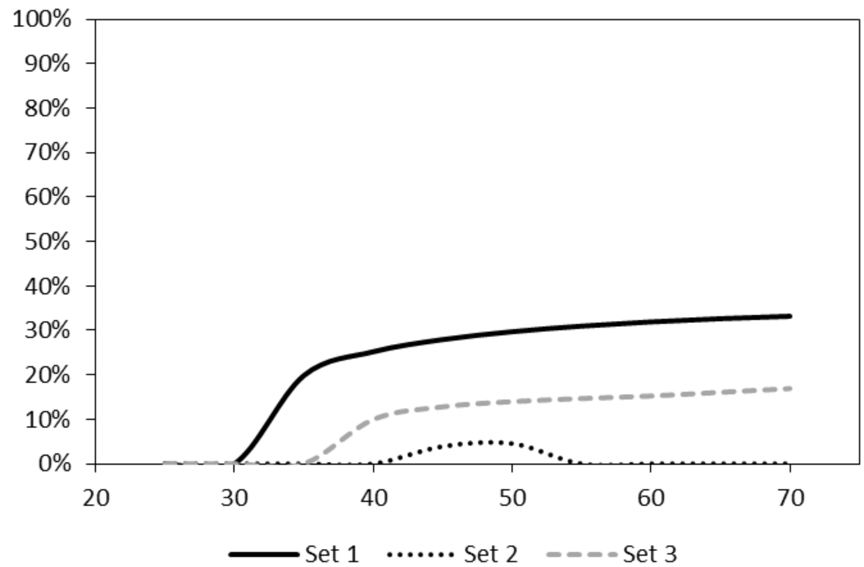

Figure 7.2: *Implied volatilities for Nestlé generated by the parameter sets from the CIR model.*

Note that all three parameter sets implies a volatility of zero for low strikes, and that they in turn seem to increase. For parameter set 2 however, the implied volatilities shortly fall to zero again. We see that with parameter set 1 and 3 the model generates almost flat, but slightly upward sloping volatility smiles for high strikes.

7.1.2 Gamma-OU Intensity

The three chosen parameter sets from the calibration of the Gamma-OU model are presented in Table 7.2.

	$\boldsymbol{\lambda_0}$	$\boldsymbol{\theta}$	$\boldsymbol{a}$	$\boldsymbol{b}$	**ARPE**	**SSE**
Set 1	0.00023	0.015	15.48	109	9.2 %	22.75
Set 2	0.00014	0.006	15.06	40	9.9 %	23.55
Set 3	0.00007	0.005	15.45	30	10.6 %	24.87

Table 7.2: *Parameter sets selected from the calibration of the Gamma-OU model on Nestlé.*

Note that the a parameter is quite similar for all three parameter sets. However, the b parameter differs between the three. As mentioned before, b affects the jumps size of the compound Poisson process driving the intensity process. What seems to be apparent here is that apart from the compensating effect discussed earlier between a and b, reductions in θ and λ_0 also seem to compensate for a higher jump size, that is a lower b. For λ_0 the reason may be that because the intensity is bound to jump higher when it jumps, a lower starting point can compensate for this. An intuitive explanation for the differences in θ is found by recalling how the Gamma-OU process was simulated. In the simulation of a path, θ also affects the jump intensity of the Poisson process. The lower θ, the fewer jumps, and hence a higher jump size may be present.

The calculated swaption prices for the three parameter sets can be found in Figure 7.3, where we see that sets 2 and 3 generate almost identical swaption prices. On the other hand, set 1 generates swaption prices below the other two for all strikes. The higher jump size in sets 2 and 3 increases the probability of a high intensity at expiry, leading to an increased probability of a high spot CDS spread. The presence of a strong jump component was also used as an explanation for high swaption values for high strikes by Brigo & El-Bachir (2006) in the analysis of their jump extended SSRD model. The implied volatilities are shown in Figure 7.4.

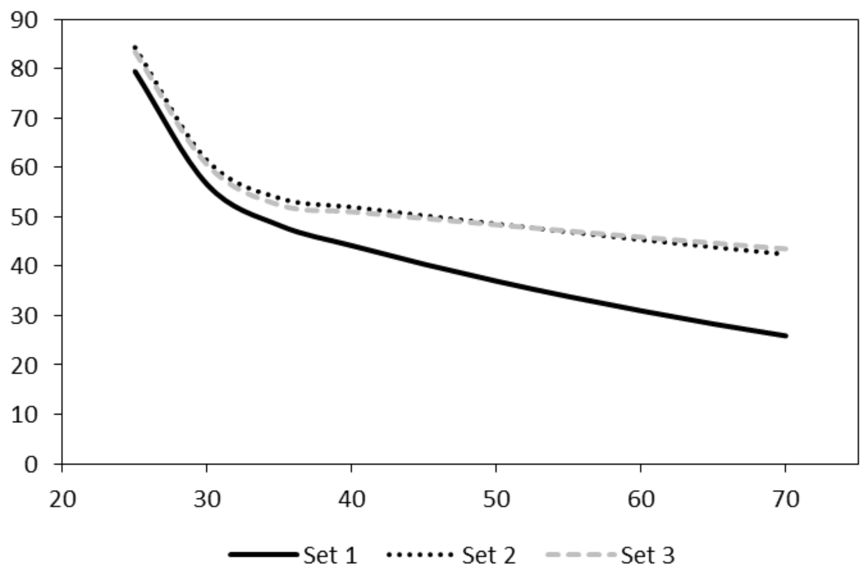

Figure 7.3: *Theoretical swaption prices for Nestlé, calculated by the Gamma-OU model. The forward spread is 43 bp.*

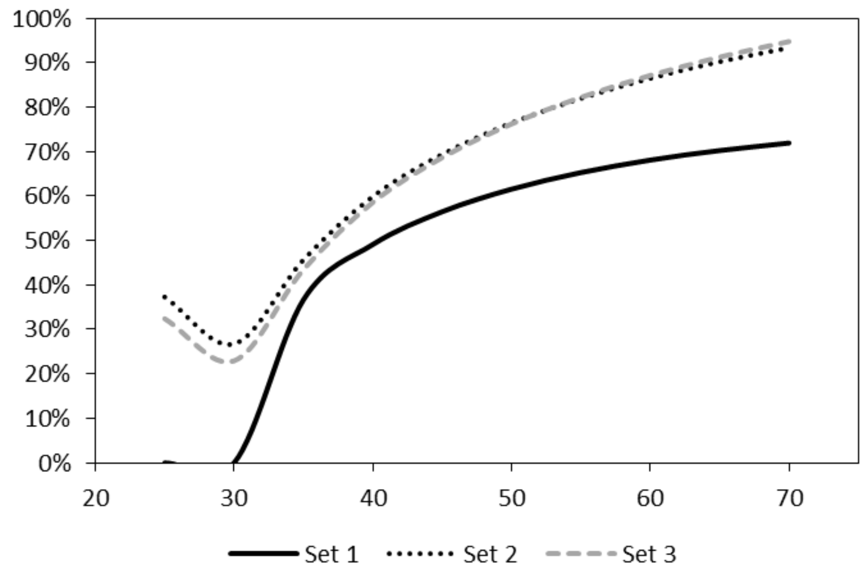

Figure 7.4: *Implied volatility smiles for Nestlé generated by the Gamma-OU model*

The implied volatility smiles for set 2 and 3 slope downwards for low strikes, before they rise sharply. The implied volatility pattern for set 1 shows some of the same features, but is clearly different for low strikes. Due to the lack of a strong jump component compared to the other two sets, the smile also seems to flatten more out for higher strikes.

7.1.3 IG-OU Intensity

Table 7.3 lists the chosen parameter sets from the IG-OU model.

	λ_0	θ	a	b	ARPE	SSE
Set 1	0.00022	0.031	1.942	28	9.2 %	22.68
Set 2	0.00023	0.003	5.332	8	9.2 %	22.91
Set 3	0.00016	0.047	6.114	129	9.6 %	23.11

Table 7.3: *Chosen parameter sets from the IG-OU model for Nestlé.*

From the calibration of the IG-OU model, three quite different parameter sets were selected. There are especially differences in a and b, but also θ and λ_o shows variation. Any clear patterns do not seem to be obvious, and as can be seen from Figure 7.5 the parameter sets produce very different swaption values.

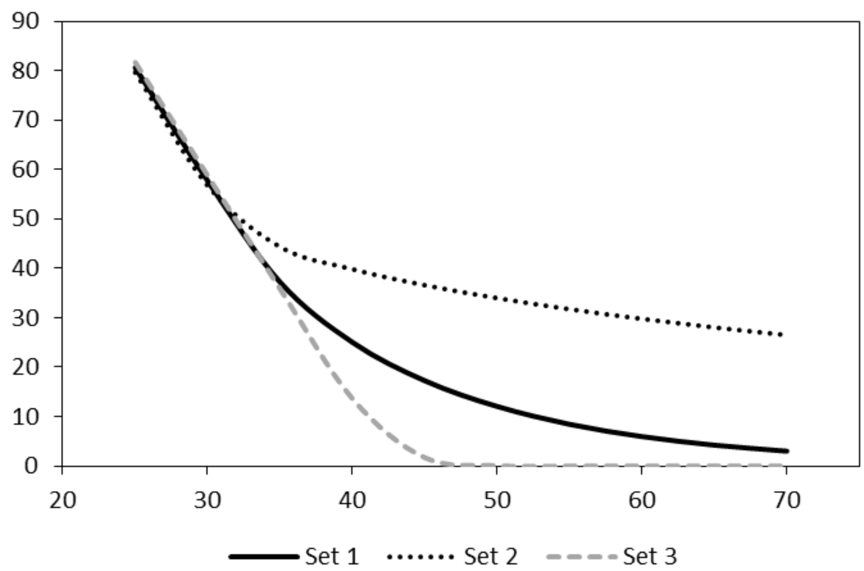

Figure 7.5: *Swaption values for Nestlé by the IG-OU model. The forward spread is 43 bp.*

It seems that a low b indicates a high swaption value for high strikes. As argued before, this may come from the fact that the value of b determines the strength of the jumps of the second part of the BDLP.

The implied volatilities generated, depicted in Figure 7.6, show the same differences. Set 1 and 2 produce upward sloping smiles, although set 1 seems to flatten out for higher strikes. Set 3 is only able to produce a small implied volatility "hump" from strikes between 40 and 60 basis points.

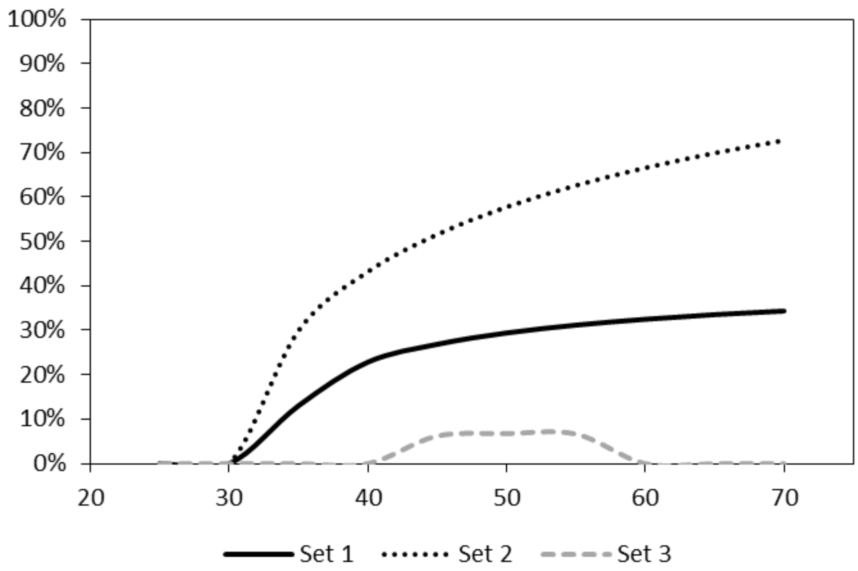

Figure 7.6: *Implied volatilities for Nestlé by the IG-OU model.*

7.1.4 Comparison of the models

In Table 7.4, the minimum, maximum and average relative difference between the parameter sets across strikes are shown. For some strikes, the relative difference is not a number due to the zero swaption value seen for some parameter sets. These are excluded in the calculations of the statistics below.

		Minimum	Maximum	Average
CIR	***Set 1 & 2***	0 %	1 058 056 %	176 979 %
	Set 1 & 3	2 %	10 401 %	2 139 %
	Set 2 & 3	2 %	183 322 %	30 765 %
Gamma-OU	***Set 1 & 2***	6 %	64 %	30 %
	Set 1 & 3	5 %	68 %	30 %
	Set 2 & 3	0 %	3 %	1 %
IG-OU	***Set 1 & 2***	1 %	782 %	239 %
	Set 1 & 3	1 %	2 147 899 %	30 9705 %
	Set 2 & 3	3 %	8066535 %	1160375 %

Table 7.4: *The minimum, maximum and average relative difference across strikes between the parameter sets.*

Clearly, for both the CIR and the IG-OU model there are huge differences in values between the parameter sets. The story is different for the Gamma model, where the difference between set 2 and 3 is quite small, confirming the impression from before. However, compared to set 1 they are both on average very different, but not nearly to the extent of the CIR and IG-OU model.

The parameter sets with the lowest sum of squared error from the three models are compared in Figure 7.7 to highlight the different features of the models. The theoretical swaption values are shown to the left, and the implied volatilities are shown to the right.

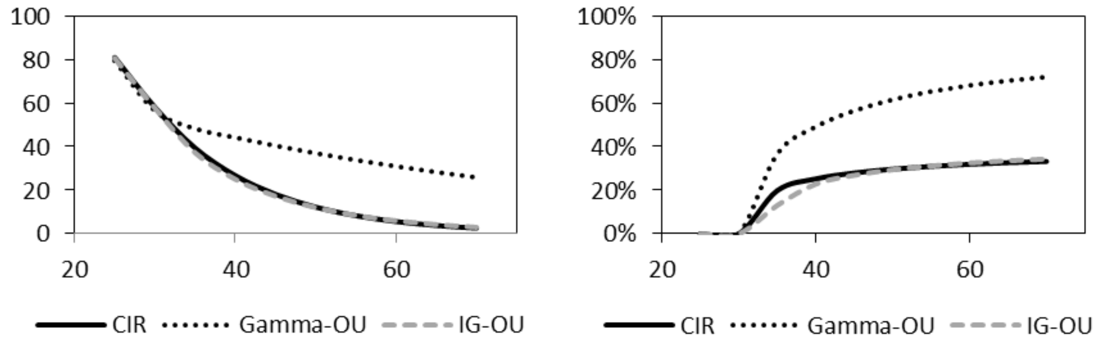

Figure 7.7: *Comparison of parameter set 1 from each of the three intensity models. The swaption values for Nestlé are depicted to the left and the implied volatilities to the right.*

Note that the CIR and IG-OU models generate quite similar swaption values, while the large jump size in the Gamma-model results in higher swaption values and implied volatilities for high strikes.

7.2 Royal Bank of Scotland

For Royal Bank of Scotland, estimates of the forward spread vary from 231 to 235 basis points. The forward spread is therefore fixed at 233 bp, and swaption values for strikes in the interval $[175 - 310]$ with steps of 15 basis points are calculated.

7.2.1 CIR Intensity

In the calibration of the CIR model on Royal Bank of Scotland, very little variation was found in the obtained parameter values. As can be seen from Table 7.5, parameter set 1 and 2 are almost identical, with only very small differences. They are both included to see whether or not differences of small size have any effect on swaption values, or if only larger differences are able to generate different swaption values. Parameter set 3 is included because of its higher volatility parameter, but as can be seen it is also a worse fit than the two other sets.

	κ	σ^2	λ_0	$\bar{\lambda}$	ARPE	SSE
Set 1	0.213	0.034	0.00434	0.0797	6.3 %	498
Set 2	0.204	0.033	0.00448	0.0818	6.2 %	499
Set 3	0.304	0.040	0.00286	0.0661	7.3 %	608

Table 7.5: Three parameter sets from the calibration of the CIR model on RBS.

In Figure 7.8 we see, not surprisingly, that parameter set 1 and 2 produce similar swaption values. What is interesting is to see that parameter set 3, with the highest volatility parameter,

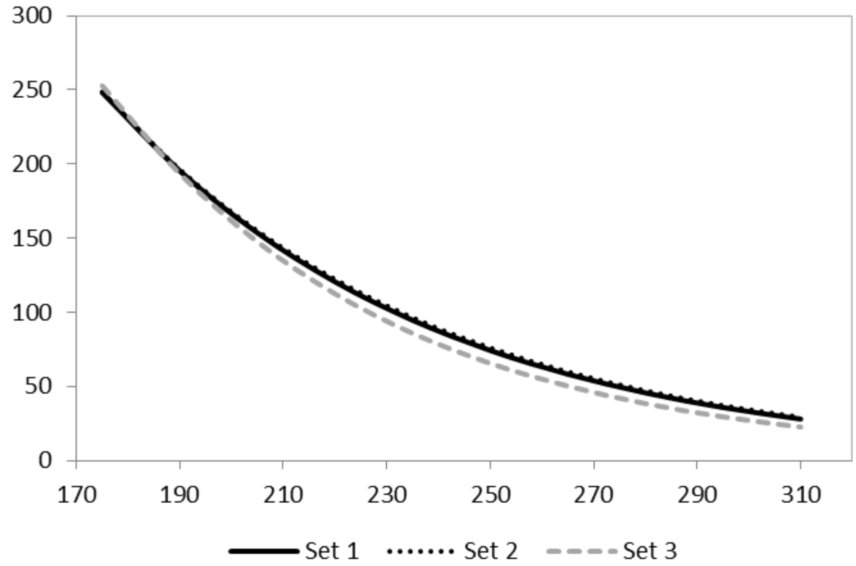

Figure 7.8: *Theoretical swaption values on RBS generated by the CIR model. The forward spread is 233 basis points.*

seems to generate lower swaption prices, although still not hugely different from the other two. Clearly a higher volatility parameter alone is not enough to observe higher swaption values. An explanation for this might be that the higher κ causes the intensity process to return to its long term mean quicker, leading to less stochasticity for the intensity process. In addition, the long term mean $\bar{\lambda}$ and the starting intensity λ_0 are lower for set 3. This may affect the swaption values in two ways. Firstly, it leads to a lower intensity, which again leads to a lower CDS spread at expiry. Secondly, through the term $\sigma\sqrt{\lambda_t}$ the lower intensity will reduce the effects of the diffusion term in the CIR process. These observations are consistent with the observations of Brigo & Cousot (2006).

The implied volatilities are shown in Figure 7.9, where the same patterns are seen. Except for a little downward sloping part for low strikes for parameter set 3, the implied volatility curve for all parameter sets are only very slightly upwards sloping.

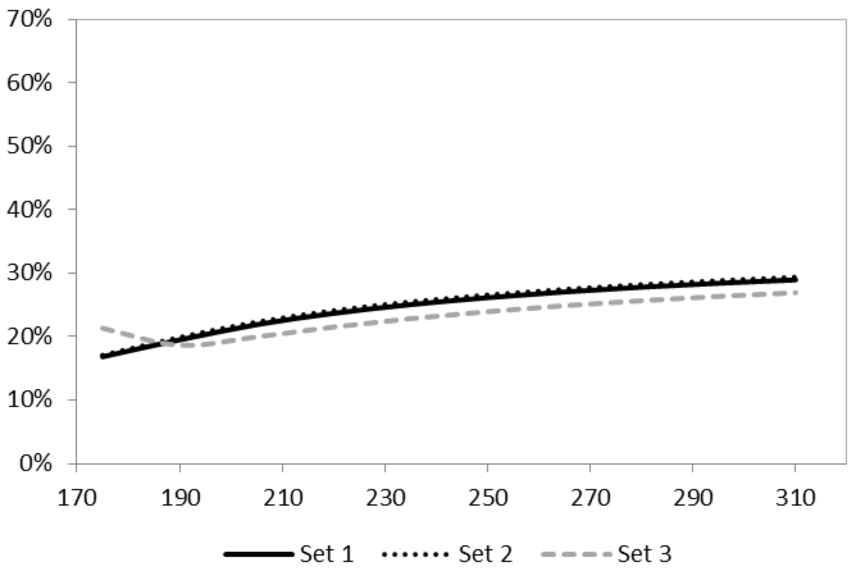

Figure 7.9: *Implied volatilities for RBS by the CIR model.*

7.2.2 Gamma-OU Intensity

Three chosen parameter sets for from the calibration of the Gamma-OU model can be found in Table 7.9. Comparing parameter set 1 and 2, the aforementioned compensating effect between a and b is evident. There are only small differences in λ_0 and θ between the sets, but great differences in a and b. In parameter set 3, we once again see different parameter values for a and b, in addition to a different θ, compared to the other sets.

	$\boldsymbol{\lambda_0}$	$\boldsymbol{\theta}$	$\boldsymbol{a}$	$\boldsymbol{b}$	**ARPE**	**SSE**
Set 1	0.00411	0.2852	1555	24550	6.5 %	534
Set 2	0.00412	0.2752	6.924	105.14	6.5 %	541
Set 3	0.00404	0.1211	1.236	8.29	6.7 %	612

Table 7.6: *Parameter sets from the Gamma-OU model calibrated to market quotes on RBS.*

Figure 7.10 displays the swaption values. The effect of the low jump size in set 1 causes the intensity to not be able to reach a level where the CDS spread is above 250 basis points, regardless of the large number of jumps by the compound Poisson process driving the intensity process. Set 2 on the contrary, with fewer jumps of larger size, is able to generate non-zero swaption prices for all strikes. Finally, note the large differences in swaption values when we compare with parameter set 3, where the large jump size leads to very high swaption values.

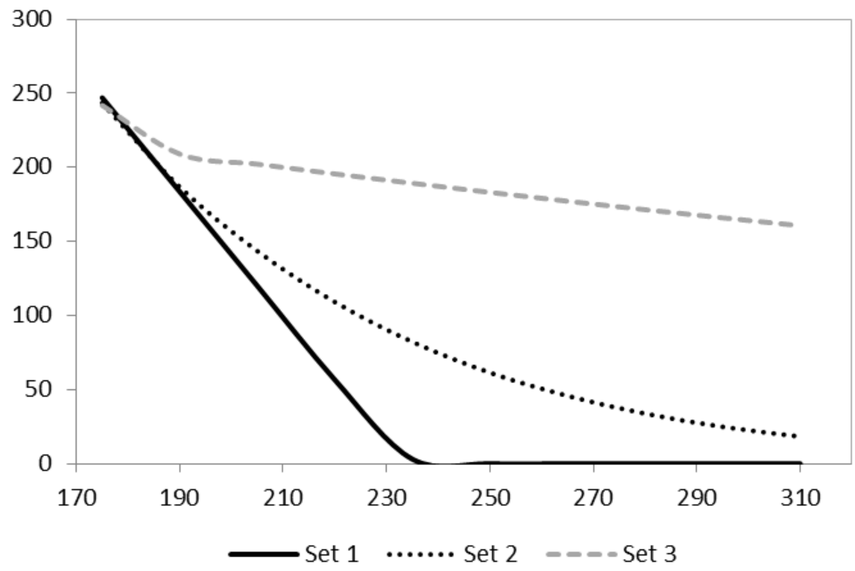

Figure 7.10: *Swaption values for RBS, by the Gamma-OU model. The forward spread is 233 bp.*

The implied volatility smiles generated by the Gamma-OU model can be found in Figure 7.11.

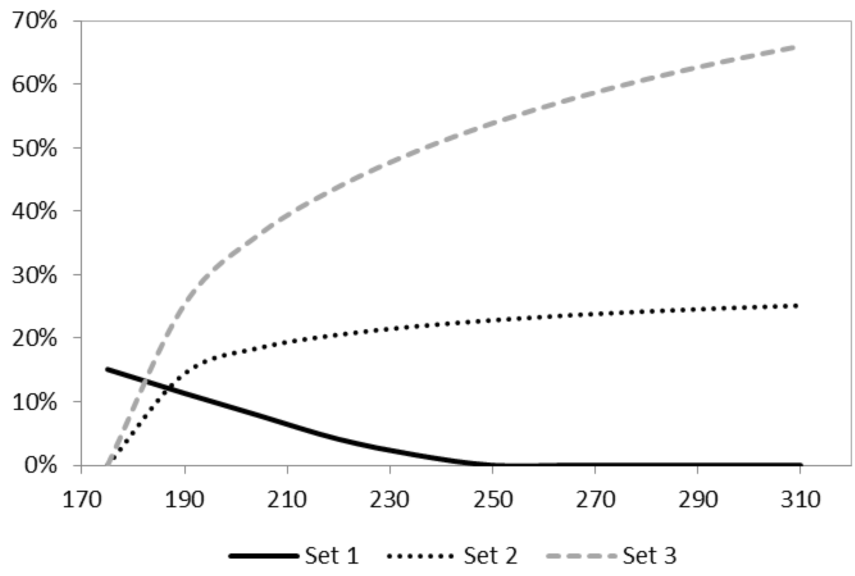

Figure 7.11: *Implied volatility smiles generated by the Gamma-OU model.*

Interestingly, but not surprisingly, parameter set 1 shows a downward sloping implied volatility pattern, while implied volatilities for set 2 slope upwards. This suggests that the power of the jump component, in terms of jump size, determines in which direction the smile slopes. Parameter set 3 clearly differs from them both in terms of the level of implied volatility, and the high jump size creates a smile which seems to keep on increasing quite rapidly as opposed to the smile from set 2 which flattens out for high strikes.

7.2.3 IG-OU Intensity

Table 7.7 shows the selected parameter sets from the calibration of the IG-OU model on Royal Bank of Scotland.

	$\boldsymbol{\lambda_0}$	$\boldsymbol{\theta}$	$\boldsymbol{a}$	$\boldsymbol{b}$	**ARPE**	**SSE**
Set 1	0.00411	0.2852	60	953	6.5 %	534
Set 2	0.00411	0.2849	3.3	51.4	6.5 %	534
Set 3	0.00411	0.2765	0.8	12.2	6.5 %	539

Table 7.7: *Selected parameter sets from the calibration of the IG-OU model on RBS.*

The parameter sets offer an interesting example where the influence of the compensating effect between a and b on swaption values can be investigated. While λ_0 and θ are stable across the parameter sets, a and b differ greatly, where a high a seems to be followed by a high b. The effect of this on swaption values can be seen in Figure 7.12.

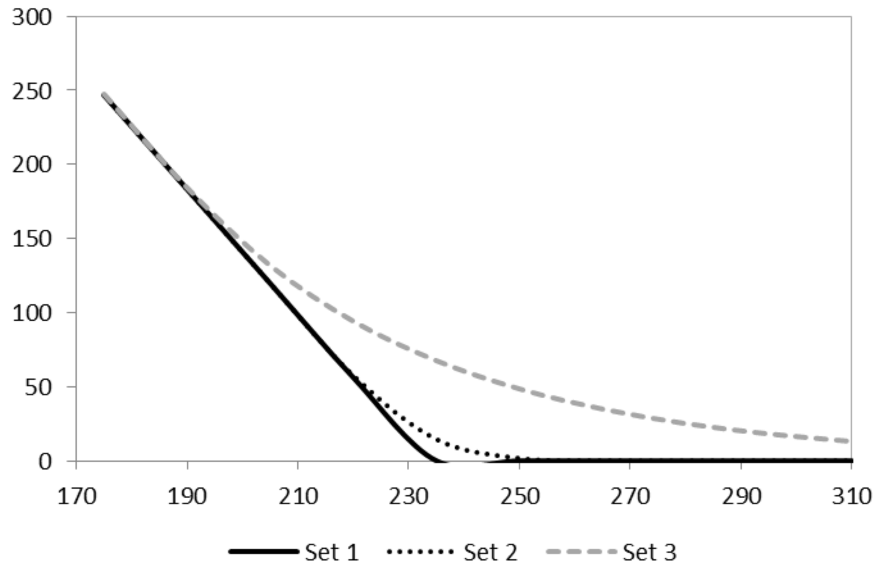

Figure 7.12: *Swaption values on RBS by the IG-OU process. The forward spread is 233 bp.*

Despite their large differences in a and b the swaption values generated by set 1 and 2 are quite similar up to a strike of 220 bp. Thereafter an interval of large relative differences is seen, before they both yield swaption values of zero. On the other hand, due to the strong jump component, values from set 3 show a less steep decline for higher strikes, yielding positive values for all strikes. The corresponding implied volatilities are depicted in Figure 7.13.

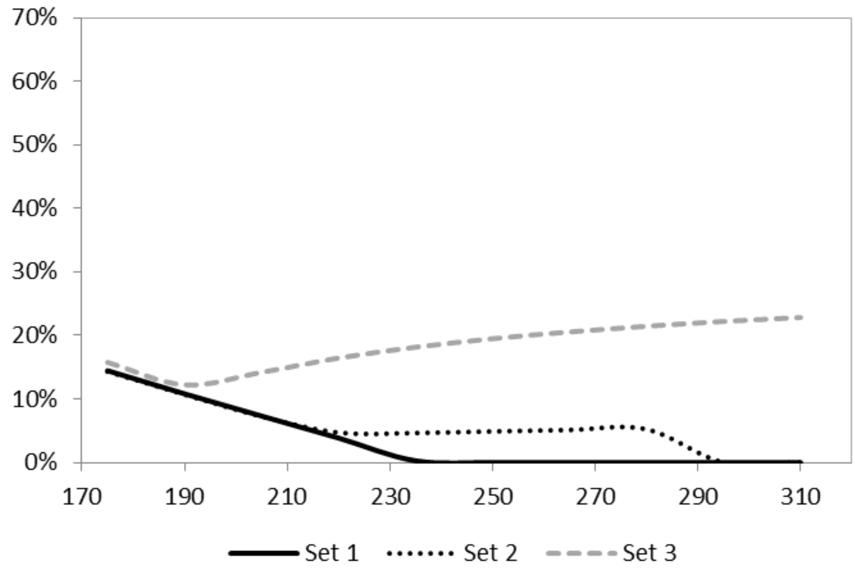

Figure 7.13: *Implied volatilities for RBS, generated by the IG-OU model.*

All three implied volatility smiles are downward sloping for low strikes. While set 3 goes slightly upwards as the strike increases, set 1 continues to slope down and reach zero when swaption prices reach zero. Set 2 shows an almost constant implied volatility for strikes between 220 and 280, before they continue down towards zero.

7.2.4 Comparison of the Models

The relative difference measures are shown in Table 7.8. As expected, the smallest differences are seen for the CIR model. This is due to the fact that in the calibration, large differences in parameters were not found.

		Minimum	Maximum	Average
CIR	***Set 1 & 2***	0 %	4 %	2 %
	Set 1 & 3	1 %	24 %	12 %
	Set 2 & 3	1 %	29 %	14 %
Gamma-OU	***Set 1 & 2***	2 %	2 606 %	544 %
	Set 1 & 3	2 %	6 132 %	1 293 %
	Set 2 & 3	1 %	781 %	251 %
IG-OU	***Set 1 & 2***	0 %	2 694 720 %	538 944 %
	Set 1 & 3	0 %	12 572 855 %	2 514 587 %
	Set 2 & 3	0 %	775 018 %	101 406 %

Table 7.8: *The minimum, maximum and average relative difference in swaption prices across strikes between the parameter sets.*

The table shows a different story for Gamma-OU and the IG-OU model, where we see large differences for both, confirming the impression from above. The apparent similarity in swaption prices between set 1 and 2 from the IG-OU model is discarded by a high maximum and average relative difference. These numbers are amplified by the division on a low number and the fact that the equal swaption prices of zero are not included in the calculation of the average relative difference.

Also for swaptions written on the Royal Bank of Scotland, the swaption values and implied volatilities generated by the parameter sets which give the smallest SSE from each model are compared in Figure 7.14.

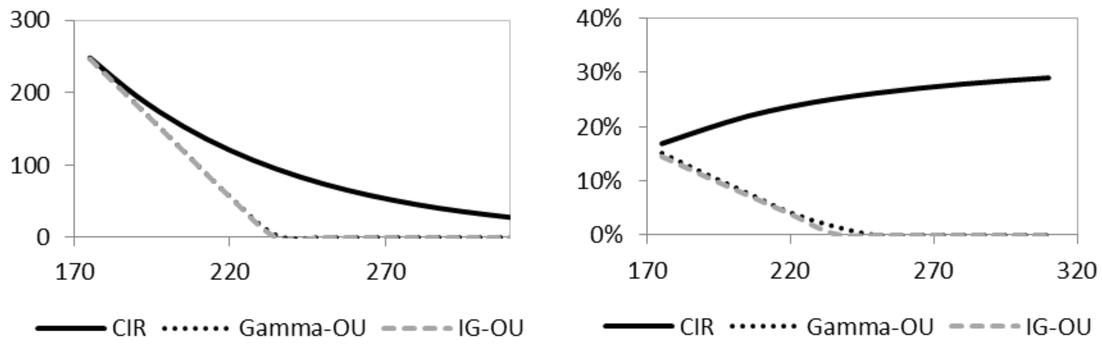

Figure 7.14: *Comparison of parameter set 1 from each of the three models. Forward spread is 233 bp.*

Interestingly, parameter set 1 from the calibration of Gamma-OU and IG-OU produce close to identical swaption values except for a strike of 235 bp, not easily seen in the figure. However, they both generate zero values for higher strikes and downward sloping volatility smiles, something that is not very realistic. The CIR process on the other hand gives non-zero swaption values for all strikes in addition to an upward sloping volatility smile in the case of Royal Bank of Scotland.

7.3 National Bank of Greece

Lastly, the case of National Bank of Greece, the company with the lowest perceived credit quality in the data set, is investigated. The level of the CDS spreads written on NBG is very different from the two other companies, and as opposed to them the term structure is downward sloping. The forward spread is fixed at 930 basis points, and for all models prices for strikes in the interval $[700 - 1150]$ with steps of 50 bp is calculated.

7.3.1 CIR Intensity

The selected parameter sets from the calibration of the CIR model can be found in Table 7.9.

	κ	σ^2	λ_0	$\bar{\lambda}$	ARPE	SSE
Set 1	0.653	0.220	0.241	0.168	1.4 %	4740
Set 2	0.816	0.041	0.250	0.146	1.5 %	5660
Set 3	0.881	0.300	0.247	0.170	1.6 %	5716

Table 7.9: *The parameter sets selected to value swaptions with the CIR model, written on National Bank of Greece.*

Note the high starting intensity, and the decreasing drift through the lower long term mean parameter, reflecting the decreasing CDS spreads. Once again differences in the volatility parameter are found. Earlier it was argued that a high volatility parameter would, everything else equal, increase swaption values. It was also suggested that a high value of κ would decrease the stochasticity of the intensity process, reducing the value of the swaption. Comparing parameter set 1 and 3, we see that λ_0 and $\bar{\lambda}$ are similar, but there are differences in κ and σ^2. Parameter set 3 has the highest σ^2, but also the highest κ. This case is then another example of these two effects battling each other. Parameter set 2 exhibits a very low volatility compared to the two other sets, and compared to set 1 also a high speed of mean reversion, meaning that relatively low swaption values are expected.

The corresponding swaption values generated by the parameter sets are shown in Figure 7.15.

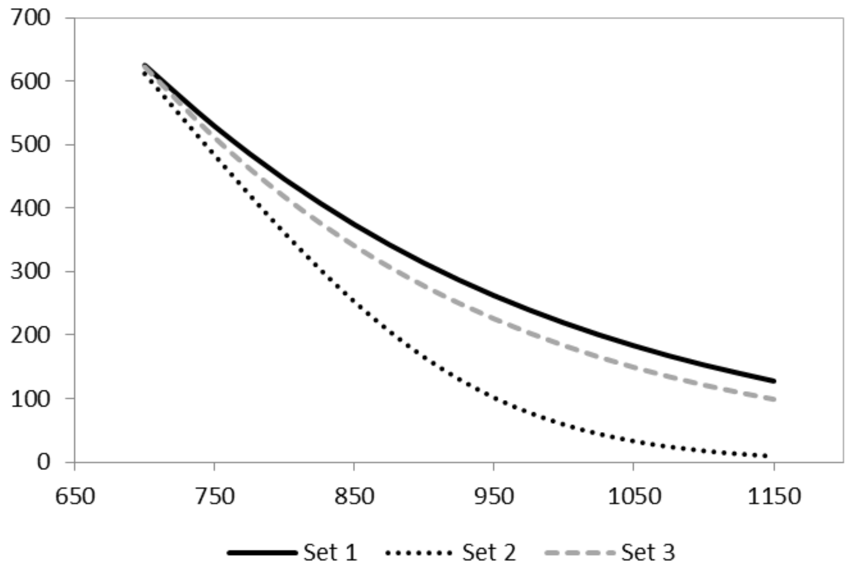

Figure 7.15: *Swaption prices for NBG, by the CIR model. Forward spread is 930 bp.*

Despite of the higher volatility parameter in parameter set 3, parameter set 1 yields greater swaption values due to its lower speed of mean reversion. As expected parameter set 2 generates low swaption values compared to the other sets. The swaption values translated into implied volatilities are depicted in Figure 7.16.

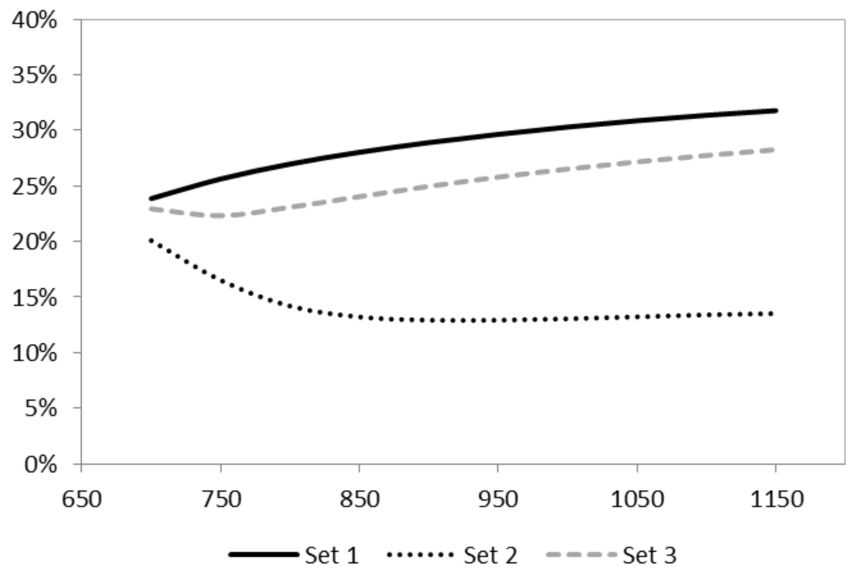

Figure 7.16: *Implied volatilites for swaptions on NBG, generated by the CIR model.*

Interestingly, we see that the CIR model is able to generate both upward sloping and downward sloping implied volatility smiles, depending on which parameters are used. The jump extended SSRD model investigated by Brigo & El-Bachir (2006) also generated both upwards and downwards sloping volatility smiles for different parameter values. They explained the occurrence of an upward sloping smile as a result of the included jump component. From Figure 7.16 we see that also without the extension of shifts and jumps, the square root diffusion model, which is the CIR model, can generate both somewhat upward sloping and downward sloping volatility patterns. However, for high strikes they are all quite flat.

7.3.2 Gamma-OU Intensity

Parameters selected from the calibration are shown in Table 7.10.

	λ_0	θ	a	b	ARPE	SSE
Set 1	0.185	1.032	0.160	0.174	1.2 %	3282
Set 2	0.154	0.864	0.166	0.064	1.5 %	3761
Set 3	0.244	0.729	2.034	13.50	1.5 %	5267

Table 7.10: *The parameter sets for the Gamma-OU model used to value swaptions written on the National Bank of Greece.*

Comparing the three parameter sets, we note that there are differences in almost every parameter value, except for the similar value of a in parameter set 1 and 2. We also see that the ranges of a and b are quite wide, but one should also note that the third parameter set has a higher SSE than the two other. The resulting swaption prices can be seen in Figure 7.17.

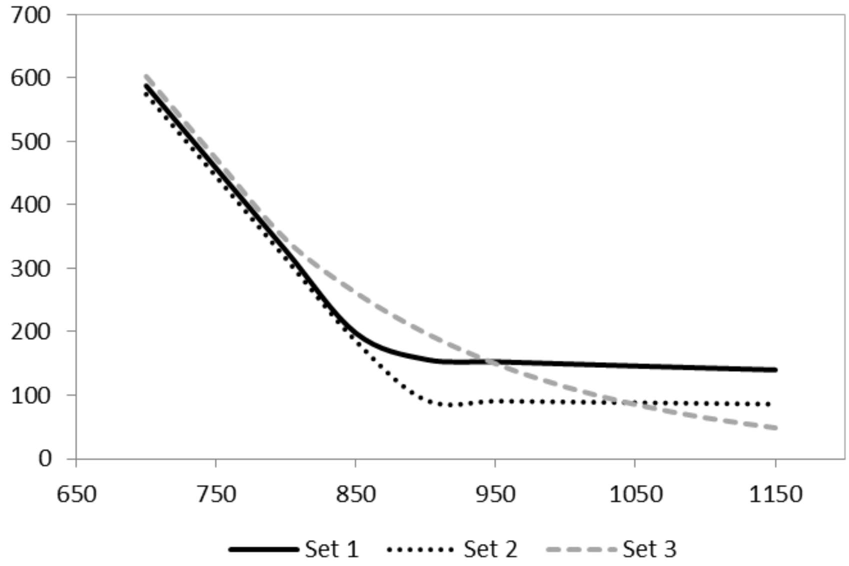

Figure 7.17: *NBG swaption values, calculated by the Gamma-OU intensity model. The forward spread is 930 bp.*

The shape of the curves for parameter sets 1 and 2 are similar, and they both flatten out for high strikes. This is probably due to their large jump size, where a jump leads to a high intensity and thereby a high CDS spread. However, they differ for which strikes they flatten out, causing a difference of around 60 basis points for high strikes. On the contrary, due to its lack of large jumps, parameter set 3 shows a steady decline in swaption values when the strike increases. The implied volatility smiles are shown in Figure 7.18

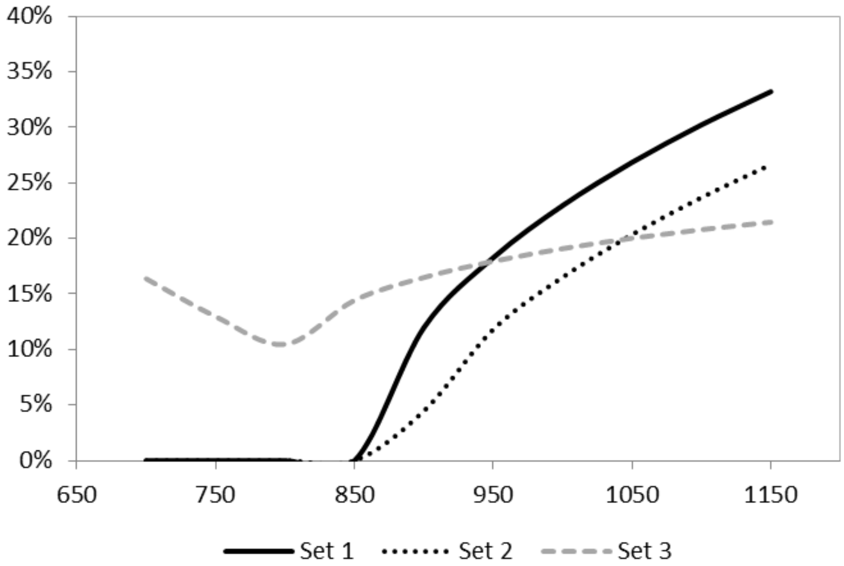

Figure 7.18: *Implied volatility smiles for swaption prices on NBG from the Gamma-OU model.*

As for the swaption values, set 1 and 2 show similar shapes at different levels, and the implied volatilities are rapidly increasing for higher strikes due to the strong jump component. The implied volatility smile generated by set 3 is downward sloping for low strikes, before it slopes up, although less steeply than for the two first parameter sets.

7.3.3 IG-OU Intensity

Selected parameters from the IG-OU model are presented in Table 7.11.

	λ_0	θ	a	b	ARPE	SSE
Set 1	0.220	0.908	0.214	0.406	1.3 %	4186
Set 2	0.211	0.896	0.208	0.035	1.3 %	4321
Set 3	0.245	0.689	1.295	9.340	1.5 %	5383

Table 7.11: *The IG-OU parameter sets selected to value National Bank of Greece swaptions.*

It is of special interest to notice the differences between sets 1 and 2. They are comparable in λ_0, θ and a, but set 2 has a lower value of b. Parameter set 3 has higher values of λ_0, a and b, but also a lower value of θ, and it is also a worse fit than the two other parameters sets. The corresponding theoretical swaption values are presented in Figure 7.19.

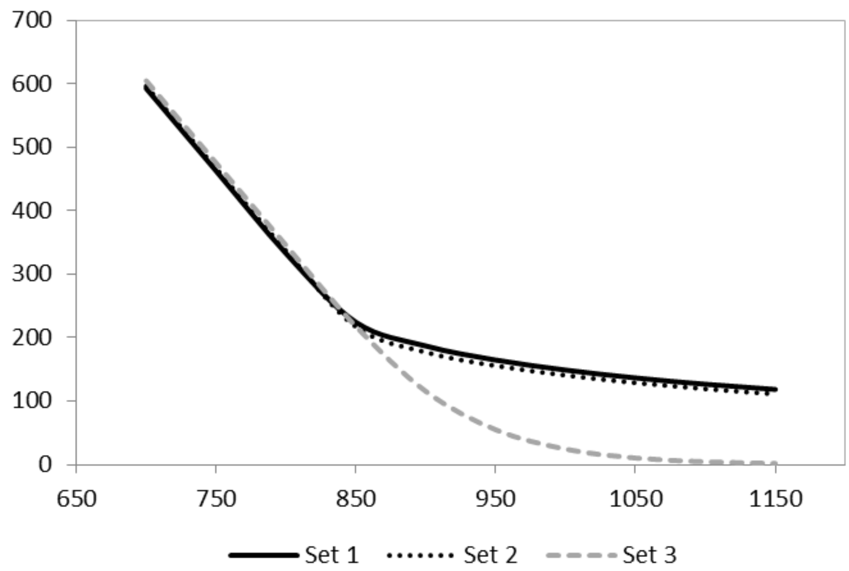

Figure 7.19: *Swaption values for NBG, calculated by the IG-OU model. Forward spread is 930 bp.*

Here the parameter sets that are comparable in terms of λ_0, θ and a but differ in b, that is parameter set 1 and 2, manage to generate swaption prices with small relative differences. Parameter set 3 fails to produce similar values, falling very low for high strikes.

The implied volatility smiles generated by the IG-OU model values can be seen in Figure 7.20.

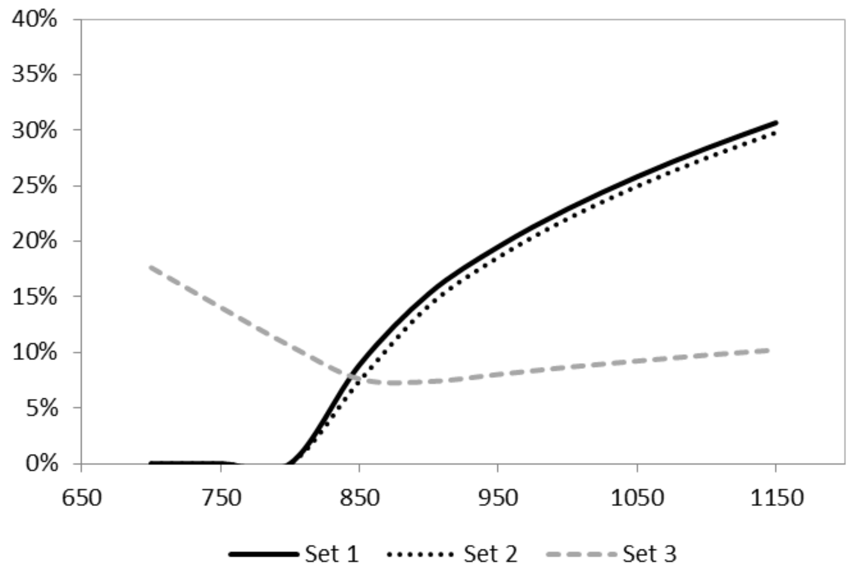

Figure 7.20: *Implied volatilities for the three chosen parameter sets from the IG-OU model. Reference entity is National Bank of Greece.*

Also here, the jump only intensity model is able to generate quite steep upwards sloping volatility smiles. But again, the ability to do so seems to depend on the size of the jump component, as set 3 produces slightly u-curved smiles, with a less steep upward slope.

7.3.4 Comparison of the Models

Table 7.12 shows the minimum, maximum and average relative differences across strikes for the parameter sets calibrated to National Bank of Greece market data.

		Minimum	Maximum	Average
CIR	***Set 1 & 2***	2 %	1 313 %	314 %
	Set 1 & 3	0 %	29 %	15 %
	Set 2 & 3	2 %	995 %	239 %
Gamma-OU	***Set 1 & 2***	2 %	70 %	41 %
	Set 1 & 3	2 %	187 %	48 %
	Set 2 & 3	3 %	115 %	38 %
IG-OU	***Set 1 & 2***	1 %	7 %	4 %
	Set 1 & 3	2 %	6 141 %	1 087 %
	Set 2 & 3	0 %	5 756 %	1 018 %

Table 7.12: *The minimum, maximum and average relative difference across strikes for the parameter sets.*

As a result of higher values in general, the relative differences are smaller in this case, but also here they are quite large for many of the parameter sets. The best performer in terms of variation between two parameter sets is the IG-OU model, but it is also the worst.

An illustration of the swaption values and implied volatilities generated by the parameter set with the lowest SSE from each model is presented in Figure 7.21.

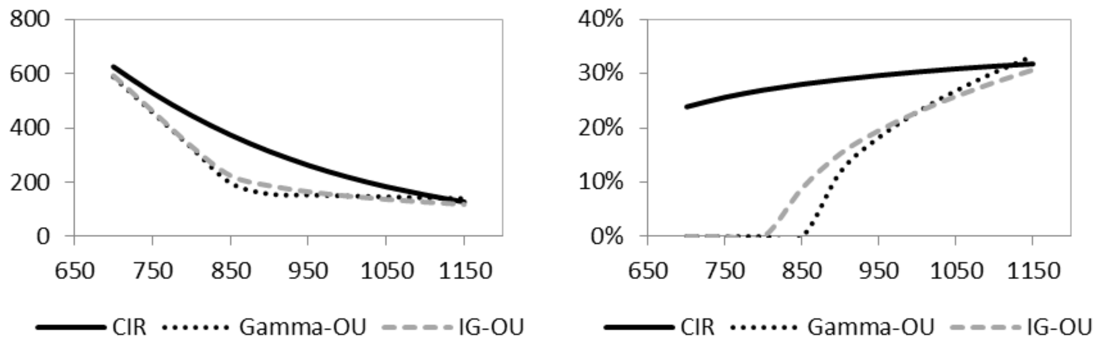

Figure 7.21: *A comparison of swaption values and implied volatilities from the three models. Forward spread is 930 bp.*

As was the case for Royal Bank of Scotland, also for National Bank of Greece the Gamma-OU model and IG-OU produce seemingly quite similar swaption values, and they both produce a sharply increasing volatility smile. The CIR process on the other hand shows a steadier decline in swaption values, resulting in a more flat volatility smile, but still slightly upward sloping. Also, the CIR process almost consistently generates higher swaption values than the two jump processes in the case of National Bank of Greece.

8 Concluding Remarks

The topic of this thesis was to investigate the suitability of valuing credit default swaptions with the use of stochastic intensity models calibrated to CDS market quotes. In particular, we focused on three stochastic intensity models; the CIR model, the Gamma Ornstein-Uhlenbeck model and the Inverse Gaussian Ornstein-Uhlenbeck model.

The investigation of the models was threefold. First, the difference in the parameters obtained in the calibration was examined, where possible explanations for the appearance of different model parameters were discussed. Next, the impact of these different parameters on swaption values were illustrated and quantified. In addition, the models' capacity in generating plausible volatility smiles was reviewed.

Except in one case for the CIR model, quite large differences were found in a selection of fitted parameters of the models. Especially for the Gamma- and IG-OU models, the variation in some of the model parameters was substantial, explained by the specification of the background driving Lévy process. This illustrates that the choice of starting values indeed may have a large impact on which model parameters are found, indicating that the possibility of specifying the model wrongly is present.

The diversity was reflected in the swaption values calculated on the basis of the selected parameter sets, where great relative differences were seen for the most part. Only in one case for each model, two sets of parameters calculated swaption values of acceptable average relative difference. In addition, several examples were seen where some of the fitted parameters returned swaption values of zero for high strikes, an issue observed for all of the three models. When comparing the swaption prices calculated by the parameter set with the lowest sum of squared error from each model, the CIR model had a tendency to yield higher values for a given strike than the jump models for two of three reference entities. Another distinction between the diffusion model and the jump models was the steady decline in values as the strike increased for the former, while the latter showed patterns where the swaption values decreased less for higher strikes. This attribute was connected with the presence of a strong jump component, and also translated into a steeper upward sloping implied volatility smiles compared to the CIR model.

With respect to the implied volatility smiles, several shapes were seen depending on the parameters. As inferred from previous papers on the subject, an upward sloping volatility smile was deemed plausible. This was not always present in the swaption prices calculated, as also u-curves, hump-curves and downward sloping curves were seen.

It is difficult to say something exact about the three stochastic intensity models' ability to generate realistic swaption values or implied volatilities, due to the lack of market data. What can be concluded from the above analysis, however, is that when calibrating the three intensity models to CDS market quotes, the potential for obtaining the wrong price is clearly present. Great caution must therefore be taken. A further analysis on the matter could be interesting, and especially an investigation into the differences in swaption values for swaptions of longer and shorter expiry.

9 References

Ahrens, J.H. & Dieter, U. (1974) Computer methods for sampling from the gamma, beta, Poisson, and binomial distributions. *Computing,* vol. 12, pp. 223-246.

Altman, E.I., Brooks, B., Resti, A. & Sironi, A. (2005) The Link between Default and Recovery Rates: Theory, Empirical Evidence, and Implications. *The Journal of Business*, vol. 78(6), pp. 2203-2228.

Barndorff-Nielsen, O. & Shepard, N. (2001) Non-Gaussian Ornstein-Uhlenbeck-based models and some of their uses in financial economics. *Journal of the Royal Statistical Society: Series B (Statistical Methodology)*, vol. 63(2), pp. 167–241.

Bielecki, T.R., Jeanblanc, M. & Rutkowski, M. (2011) Hedging of credit default swaptions in the CIR default intensity model. *Finance and Stochastics,* vol. 15(3), pp. 541 – 572.

Black, F. (1976) The pricing of commodity contracts. *Journal of Financial Economics,* vol. 3(1), pp. 167-179.

Black, F. & Cox, J.C. (1976) Valuing Corporate Securities: Some Effects of Bond Indenture Provisions. *Journal of Finance,* vol. 31(2), pp.351-367.

Black, F. & Scholes, M. (1973) The Pricing of Options and Corporate Liabilities. *Journal of Political Economy,* vol. 81(3), pp. 637–654.

Bomfim, A.N. (2005) *Understanding Credit Derivatives and Related Instruments.* San Diego, Elsevier Academic Press.

Brigo, D. (2005) Market models for CDS options and callable floaters. *Risk*. January, pp. 89-94.

Brigo, D. & Alfonsi, A. (2005) Credit Default Swaps Calibration and Option Pricing with the SSRD Stochastic Intensity and Interest-Rate Model. *Finance and Stochastics,* vol. 9(1)

Brigo, D. & Cousot, L. (2006) The stochastic intensity SSRD model implied volatility patterns for credit default swap options and the impact of correlation. *International Journal of Theoretical and Applied Finance,* vol. 9 (3), pp. 315-339.

Brigo, D. & El-Bachir, N. (2006) Credit Derivatives Pricing with a Smile-Extended Jump Stochastic Intensity Model. *ICMA Centre Discussion Papers in Finance DP2006-13.*

Brigo, D. & El-Bachir, N. (2007) An exact formula for default swaptions' pricing in the SSRDJ stochastic intensity model. *ICMA Centre Discussion Papers in Finance DP2007-14.*

Cariboni, J. & Schoutens, W. (2009) Jumps in intensity models: investigating the performance of Ornstein-Uhlenbeck processes in credit risk modeling. *Metrika*, Vol.69(2), pp. 173–198.

Cox, J., Ingersoll, J. & Ross, A. (1985) A Theory of the Term Structure of Interest Rates. *Econometrica,* vol. 53(2), March, pp. 385–407.

Delbaen, F. & Schachermayer, W. (1994) A general version of the fundamental theorem of asset pricing, *Mathematische Annalen,* 300, pp. 463-520.

Duffie, D. & Singleton, K.J. (2003) *Credit Risk. Pricing, Measurement, and Management.* New Jersey, Princeton University Press.

Elizalde, A. (2005) Credit Default Swap Valuation: An Application to Spanish Firms. Available at www.abelelizalde.com.

Feller, W. (1951) Two Singular Diffusion Problems, *Annals of Mathematics,* 53, pp. 173.182.

Fishman, G.S (1996) *Monte Carlo: Concepts, Algorithms, and Applications.* New York, Springer-Verlag.

French, K.R., Baily, M.N, Campbell, J.Y., Cochrane, J.H., Diamond, D.W., Duffie, D., Kashyap, A.K., Mishkin, F.S., Rajan, R.G., Scharfstein, D.S., Shiller, R.J., Shin, H.S., Slaughter, M.J., Stein, J.C. & Stulz, R.M. (2010) *The Squam Lake report: fixing the financial system.* New Jersey, Princeton University Press.

Geske, R. (1977) The Valuation of Corporate Liabilities as Compound Options. *The Journal of Financial and Quantitative Analysis*, vol. 12(4), pp. 541-552.

Glasserman, P. (2003) *Monte Carlo methods in financial engineering.* New York, Springer.

Harrison, J.M. & Pliska, S.R. (1981) Martingales and Stochastic Integrals in the Theory of Continuous Trading. *Stochastic Processes and their Applications,* 11, pp. 215–260.

Houweling, P. & Vorst, T. (2005) Pricing default swaps: Empirical evidence. *Journal of International Money and Finance*, 24, pp. 1200–1225.

Hull, J.C. & White, A. (2000) Valuing Credit Default Swaps II: Modeling Default Correlations. Working paper, University of Toronto.

ISDA. (2003) Credit Derivatives Definitions. *International Swaps and Derivatives Association.*

Jamshidian, F. (2004) Valuation of credit default swaps and swaptions. *Finance and Stochastics,* vol. 8(3), pp. 343-371.

Jarrow, R.A. & Protter, P. (2004) Structural versus reduced form models: a new information based perspective. *Journal of Investment Management*, vol. 2(2), pp. 1-10.

Jarrow, R.A. & Turnbull, S.M. (1995) Pricing Derivatives of Financial Securities Subject to Credit Risk. *Journal of Finance*, vol. 50(1), pp. 53-85.

Jarrow, R.A. & Yu, F. (2001) Counterparty Risk and the Pricing of Defaultable Securities. *The Journal of Finance*, vol. 56(5), pp. 1765-1799.

Jeanblanc, M. & Rutkowski, M. (2002) Default Risk and Hazard Process. In H. Geman, D. Madan, S.R. Pliska and T. Vorst (Eds.), *Mathematical Finance – Bachelier Congress 2000.* New York, Springer, pp. 281-312.

Jönsson, H. & Schoutens, W. (2008) Single name credit default swaptions meet single sided jump models. *Review of Derivatives Research*, 11, pp. 153-169.

Kokholm, T. & Nicolato, E. (2010) Sato Processes in Default Modelling. *Applied Mathematical Finance*, vol. 17(5), October, pp. 377–397.

Kritzman, M. (1991) What Practitioners Need to Know About Estimating Volatility: Part 1. *Financial Analysts Journal*, vol. 47(4), pp. 22-25.

Lando, D. (1998) On Cox Processes and Credit Risky Securities. *Review of Derivatives Research*, vol. 2, pp. 99-120.

Lando, D. (2004) *Credit Risk Modeling: Theory and Applications.* New Jersey, Princeton University Press.

Merton, R.C (1973) Theory of Rational Option Pricing. *The Bell Journal of Economics and Management Science*, vol. 24(1), pp. 141-183.

Merton, R.C (1974) On the pricing of corporate debt: the risk structure of interest rates. *Journal of Finance*, vol. 29(2), pp. 449-470.

Michael, J.R., Schucany, W.R., & Haas, R.W. (1976) Generating random variates using transformations with multiple roots. *American Statistician,* vol. 30, pp. 88-90.

Nicolato, E. & Venardos, E. (2003) Option Pricing in Stochastic Volatility Models of the Ornstein-Uhlenbeck Type. *Mathematical Finance*, Vol.13(4), October, pp. 445 – 466.

O'Kane, D. (2008) *Modelling Single-name and Multi-name Credit Derivatives*. Chichester, John Wiley & Sons Ltd.

O'Kane, D. and Turnbull, S. (2003) Valuation of Credit Default Swaps. *Lehman Brothers Quantitative Credit Research,* 2003(Q1/Q2).

Rutkowski, M. & Armstrong, A. (2009) Valuatin of Credit Default Swaptions and Credit Default Index Swaptions. *International Journal of Theoretical and Applied Finance,* vol. 12(7), pp. 1027-1053.

Schönbucher, P.J. (2003) *Credit Derivatives Pricing Models*. Chichester, John Wiley & Sons Ltd.

Schönbucher, P.J. (2004) A measure of survival. *Risk.* August, pp. 79-85.

Scott, L.O. (1996) Simulating a multi-factor term structure model over relatively long discrete time periods, *Proceedings of the IAFE First Annual Computational Finance Conference,* Graduate School of Business, Stanford University.

Zhang, S. & Zhang, X. (2008) Exact Simulation of IG-OU Processes. *Methodology and Computing in Applied Probability*, vol. 10, pp. 337-355.

Zhou, C. (1997) A Jump-Diffusion Approach to Modeling Credit Risk and Valuing Defaultable Securities. *Finance and Economics Discussion Series,*1997(15), Board of Governors of the Federal Reserve System.

10 Appendix

10.1 Credit Default Swaption Values

Values CIR - Nestlé

	Set 1		Set 2		Set 3	
Strike	**Value**	**MC-Error**	**Value**	**MC-Error**	**Value**	**MC-Error**
25	80.95	*(.57)*	81.09	*(.08)*	79.68	*(.26)*
30	58.05	*(.57)*	58.18	*(.08)*	56.76	*(.27)*
35	39.39	*(.54)*	35.26	*(.08)*	34.25	*(.26)*
40	26.73	*(.48)*	12.52	*(.08)*	16.35	*(.22)*
45	18.12	*(.41)*	.48	*(.02)*	6.37	*(.14)*
50	12.27	*(.35)*	.0012	*(.0009)*	2.13	*(.09)*
55	8.32	*(.29)*	-	-	.63	*(.05)*
60	5.65	*(.24)*	-	-	.18	*(.03)*
65	3.84	*(.20)*	-	-	.06	*(.02)*
70	2.61	*(.17)*	-	-	.02	*(.01)*

Values Gamma-OU - Nestlé

	Set 1		Set 2		Set 3	
Strike	**Value**	**MC-Error**	**Value**	**MC-Error**	**Value**	**MC-Error**
25	79.44	*(1.45)*	84.28	*(2.37)*	83.42	*(2.56)*
30	56.52	*(1.45)*	61.37	*(2.37)*	60.51	*(2.57)*
35	48.26	*(1.41)*	53.77	*(2.35)*	52.38	*(2.55)*
40	44.17	*(1.35)*	51.97	*(2.31)*	51.01	*(2.51)*
45	40.40	*(1.30)*	50.24	*(2.27)*	49.69	*(2.48)*
50	36.97	*(1.24)*	48.56	*(2.23)*	48.39	*(2.44)*
55	33.85	*(1.19)*	46.94	*(2.19)*	47.13	*(2.41)*
60	30.97	*(1.14)*	45.38	*(2.15)*	45.90	*(2.38)*
65	28.32	*(1.09)*	43.88	*(2.12)*	44.70	*(2.34)*
70	25.90	*(1.05)*	42.42	*(2.08)*	43.53	*(2.31)*

Values IG-OU - Nestlé

Strike	Set 1 Value	MC-Error	Set 2 Value	MC-Error	Set 3 Value	MC-Error
25	80.62	*(.56)*	79.66	*(1.77)*	81.69	*(.12)*
30	57.71	*(.57)*	56.74	*(1.78)*	58.78	*(.12)*
35	37.23	*(.55)*	44.35	*(1.76)*	35.86	*(.12)*
40	25.02	*(.49)*	39.83	*(1.72)*	13.62	*(.11)*
45	17.26	*(.43)*	36.59	*(1.68)*	1.69	*(.05)*
50	12.05	*(.37)*	33.97	*(1.64)*	.06	*(.01)*
55	8.45	*(.31)*	31.73	*(1.61)*	.0004	*(.0006)*
60	5.96	*(.27)*	29.77	*(1.57)*	-	-
65	4.23	*(.23)*	28.04	*(1.54)*	-	-
70	3.01	*(.19)*	26.50	*(1.51)*	-	-

Values CIR - Royal Bank of Scotland

Strike	Set 1 Value	MC-Error	Set 2 Value	MC-Error	Set 3 Value	MC-Error
175	248.28	*(2.40)*	248.52	*(2.44)*	252.87	*(2.15)*
190	195.34	*(2.33)*	196.19	*(2.37)*	193.39	*(2.14)*
205	153.55	*(2.20)*	154.86	*(2.23)*	147.47	*(2.02)*
220	120.56	*(2.03)*	122.20	*(2.06)*	112.46	*(1.86)*
235	94.63	*(1.85)*	96.40	*(1.88)*	85.82	*(1.69)*
250	74.22	*(1.68)*	75.94	*(1.71)*	65.54	*(1.51)*
265	58.21	*(1.51)*	59.79	*(1.54)*	50.19	*(1.35)*
280	45.63	*(1.35)*	47.08	*(1.38)*	38.41	*(1.19)*
295	35.75	*(1.20)*	37.08	*(1.24)*	29.45	*(1.05)*
310	27.99	*(1.07)*	29.20	*(1.10)*	22.58	*(.93)*

Values Gamma-OU - Royal Bank of Scotland

Strike	Set 1 Value	MC-Error	Set 2 Value	MC-Error	Set 3 Value	MC-Error
175	247.09	*(.14)*	243.37	*(2.08)*	241.86	*(6.41)*
190	183.56	*(.14)*	186.72	*(2.04)*	209.02	*(6.38)*
205	120.04	*(.14)*	143.53	*(1.90)*	202.20	*(6.27)*
220	56.51	*(.14)*	109.12	*(1.72)*	195.62	*(6.15)*
235	3.04	*(.06)*	82.18	*(1.54)*	189.27	*(6.05)*
250	-	-	61.38	*(1.36)*	183.13	*(5.94)*
265	-	-	45.68	*(1.18)*	177.20	*(5.83)*
280	-	-	33.76	*(1.02)*	171.47	*(5.73)*
295	-	-	24.85	*(.88)*	165.96	*(5.63)*
310	-	-	18.23	*(.75)*	160.64	*(5.53)*

Values IG-OU - Royal Bank of Scotland

	Set 1		Set 2		Set 3	
Strike	**Value**	**MC-Error**	**Value**	**MC-Error**	**Value**	**MC-Error**
175	246.76	*(.02)*	246.70	*(.42)*	247.49	*(1.76)*
190	183.23	*(.02)*	183.16	*(.42)*	184.26	*(1.77)*
205	119.70	*(.02)*	119.63	*(.43)*	131.70	*(1.70)*
220	56.16	*(.02)*	57.48	*(.41)*	94.19	*(1.54)*
235	.0005	*(.0002)*	14.47	*(.25)*	67.53	*(1.37)*
250	-	-	1.70	*(.08)*	48.52	*(1.19)*
265	-	-	.11	*(.02)*	34.89	*(1.03)*
280	-	-	.0032	*(.0024)*	25.14	*(.88)*
295	-	-	-	-	18.15	*(.76)*
310	-	-	-	-	13.09	*(.64)*

Values CIR - National Bank of Greece

	Set 1		Set 2		Set 3	
Strike	**Value**	**MC-Error**	**Value**	**MC-Error**	**Value**	**MC-Error**
700	625	*(5.14)*	612	*(2.36)*	623	*(4.46)*
750	529	*(5.02)*	483	*(2.44)*	511	*(4.47)*
800	446	*(4.83)*	361	*(2.43)*	418	*(4.34)*
850	374	*(4.58)*	253	*(2.27)*	341	*(4.11)*
900	313	*(4.31)*	165	*(1.99)*	277	*(3.84)*
950	262	*(4.02)*	101	*(1.63)*	226	*(3.55)*
1000	219	*(3.73)*	59	*(1.27)*	184	*(3.26)*
1050	183	*(3.44)*	33	*(.95)*	149	*(2.97)*
1100	153	*(3.17)*	18	*(.68)*	121	*(2.70)*
1150	128	*(2.91)*	9	*(.48)*	99	*(2.45)*

Values Gamma-OU - National Bank of Greece

	Set 1		Set 2		Set 3	
Strike	**Value**	**MC-Error**	**Value**	**MC-Error**	**Value**	**MC-Error**
700	587	*(4.75)*	574	*(3.97)*	602	*(3.36)*
750	458	*(4.95)*	444	*(4.03)*	472	*(3.50)*
800	328	*(5.18)*	315	*(4.15)*	345	*(3.63)*
850	198	*(5.44)*	185	*(4.31)*	261	*(3.39)*
900	156	*(5.47)*	92	*(4.45)*	198	*(3.09)*
950	153	*(5.41)*	91	*(4.41)*	150	*(2.77)*
1000	149	*(5.34)*	90	*(4.37)*	113	*(2.45)*
1050	146	*(5.28)*	88	*(4.34)*	85	*(2.15)*
1100	143	*(5.22)*	87	*(4.31)*	65	*(1.88)*
1150	140	*(5.17)*	86	*(4.28)*	49	*(1.64)*

Values IG-OU - National Bank of Greece

Strike	Set 1 Value	MC-Error	Set 2 Value	MC-Error	Set 3 Value	MC-Error
700	593	*(4.42)*	596	*(4.32)*	605	*(1.49)*
750	463	*(4.62)*	466	*(4.50)*	475	*(1.55)*
800	333	*(4.84)*	337	*(4.69)*	345	*(1.61)*
850	224	*(4.97)*	217	*(4.86)*	218	*(1.64)*
900	187	*(4.84)*	177	*(4.73)*	116	*(1.45)*
950	165	*(4.70)*	156	*(4.58)*	55	*(1.09)*
1000	149	*(4.56)*	141	*(4.44)*	24	*(0.75)*
1050	137	*(4.44)*	129	*(4.31)*	10	*(0.50)*
1100	127	*(4.32)*	119	*(4.20)*	4	*(0.32)*
1150	118	*(4.22)*	111	*(4.09)*	2	*(0.21)*

10.2 Implied Volatilities

Implied Volatilities – Nestlé

	CIR			Gamma-OU			IG-OU		
Strike	**Set 1**	**Set 2**	**Set 3**	**Set 1**	**Set 2**	**Set 3**	**Set 1**	**Set 2**	**Set 3**
25	0 %	0 %	0 %	0 %	37 %	32 %	0 %	0 %	0 %
30	0 %	0 %	0 %	0 %	27 %	23 %	0 %	0 %	0 %
35	20 %	0 %	0 %	37 %	46 %	43 %	13 %	30 %	0 %
40	25 %	0 %	10 %	49 %	60 %	59 %	23 %	43 %	0 %
45	28 %	4 %	13 %	56 %	69 %	69 %	27 %	52 %	6 %
50	30 %	5 %	14 %	62 %	76 %	76 %	29 %	58 %	7 %
55	31 %	0 %	15 %	65 %	82 %	82 %	31 %	63 %	7 %
60	32 %	0 %	15 %	68 %	86 %	87 %	33 %	67 %	0 %
65	33 %	0 %	16 %	70 %	90 %	91 %	34 %	70 %	0 %
70	33 %	0 %	17 %	72 %	93 %	95 %	34 %	73 %	0 %

Implied Volatilities – Royal Bank of Scotland

	CIR			Gamma-OU			IG-OU		
Strike	**Set 1**	**Set 2**	**Set 3**	**Set 1**	**Set 2**	**Set 3**	**Set 1**	**Set 2**	**Set 3**
175	17 %	17 %	21 %	15 %	0 %	0 %	14 %	14 %	16 %
190	20 %	20 %	19 %	11 %	14 %	25 %	11 %	11 %	12 %
205	22 %	22 %	20 %	8 %	19 %	37 %	7 %	7 %	14 %
220	24 %	24 %	22 %	4 %	21 %	44 %	4 %	5 %	16 %
235	25 %	26 %	23 %	2 %	22 %	49 %	0 %	5 %	18 %
250	26 %	27 %	24 %	0 %	23 %	54 %	0 %	5 %	19 %
265	27 %	27 %	25 %	0 %	24 %	58 %	0 %	5 %	21 %
280	28 %	28 %	26 %	0 %	24 %	61 %	0 %	5 %	21 %
295	28 %	29 %	26 %	0 %	25 %	64 %	0 %	0 %	22 %
310	29 %	29 %	27 %	0 %	25 %	66 %	0 %	0 %	23 %

Implied Volatilities – National Bank of Greece

	CIR			Gamma-OU			IG-OU		
Strike	**Set 1**	**Set 2**	**Set 3**	**Set 1**	**Set 2**	**Set 3**	**Set 1**	**Set 2**	**Set 3**
700	24 %	20 %	23 %	0 %	0 %	16 %	0 %	0 %	18 %
750	26 %	17 %	22 %	0 %	0 %	13 %	0 %	0 %	14 %
800	27 %	14 %	23 %	0 %	0 %	10 %	0 %	0 %	11 %
850	28 %	13 %	24 %	0 %	0 %	14 %	9 %	7 %	8 %
900	29 %	13 %	25 %	12 %	4 %	16 %	15 %	14 %	7 %
950	30 %	13 %	26 %	18 %	12 %	18 %	20 %	19 %	8 %
1000	30 %	13 %	27 %	23 %	17 %	19 %	23 %	22 %	9 %
1050	31 %	13 %	27 %	27 %	20 %	20 %	26 %	25 %	9 %
1100	31 %	13 %	28 %	30 %	24 %	21 %	28 %	28 %	10 %
1150	32 %	14 %	28 %	33 %	27 %	21 %	31 %	30 %	10 %

10.3 Derivation of Survival Probability in the Intensity Framework

The following derivations are inspired from Lando (2004, ch. 5) from where we have that:

$$Q_t(\tau > T|\tau > t) = 1_{\{\tau>t\}} \frac{\mathbb{E}^Q\left[1_{\{\tau>T\}}|\mathcal{G}_t\right]}{\mathbb{E}^Q\left[1_{\{\tau>t\}}|\mathcal{G}_t\right]} \qquad \textbf{10.1}$$

Consider $\mathbb{E}^Q\left[1_{\{\tau>T\}}|\mathcal{G}_t\right]$. By the law of iterated expectations, we get:

$$\mathbb{E}^Q\left[1_{\{\tau>T\}}|\mathcal{G}_t\right] = \mathbb{E}^Q\left(\mathbb{E}^Q\left[1_{\{\tau>T\}}|\mathcal{G}_T\right]|\mathcal{G}_t\right) \qquad \textbf{10.2}$$

Now, consider $\mathbb{E}^Q\left[1_{\{\tau>T\}}|\mathcal{G}_T\right]$. We can write this as $Q(\tau > T|\mathcal{G}_T)$. And by the definition of τ in equation (3.5):

$$Q(\tau > T|\mathcal{G}_T) = Q\left(\int_0^T \lambda(X_s)ds < E_1 \middle| \mathcal{G}_T\right)$$

$$= 1 - Q\left(E_1 \leq \int_0^T \lambda(X_s)ds \middle| \mathcal{G}_T\right)$$

$$= 1 - \Phi_{E_1}\left(\int_0^T \lambda(X_s)ds\right)$$

where $\Phi_{E_1}(x)$ denotes the cumulative distribution function of E_1 and is given by $\Phi_{E_1}(x) = 1 - e^{-x}$. This holds because we conditioned on the information $\mathcal{G}_T$, and then $\int_0^T \lambda(X_s)ds$ is known, and E_1 is independent of $\mathcal{G}_T$. We continue and get:

$$Q(\tau > T|\mathcal{G}_T) = 1 - \left(1 - e^{-\int_0^T \lambda(X_s)ds}\right)$$

$$= e^{-\int_0^T \lambda(X_s)ds}$$

From this we keep the result that

$$\mathbb{E}^Q\left[1_{\{\tau>T\}}|\mathcal{G}_T\right] = e^{-\int_0^T \lambda(X_s)ds}$$

We insert this in (10.2) and obtain

$$\mathbb{E}^Q\left[1_{\{\tau>T\}}|\mathcal{G}_t\right] = \mathbb{E}^Q\left(e^{-\int_0^T \lambda(X_s)ds}\middle|\mathcal{G}_t\right)$$

and because $\int_0^T \lambda(X_s)ds$ is known up until time t we write

$$\mathbb{E}^Q\left[1_{\{\tau>T\}}|\mathcal{G}_t\right] = e^{-\int_0^t \lambda(X_s)ds}\mathbb{E}^Q\left(e^{-\int_t^T \lambda(X_s)ds}\middle|\mathcal{G}_t\right) \qquad \textbf{10.3}$$

And obviously

$$\mathbb{E}^Q\left[1_{\{\tau>t\}}|\mathcal{G}_t\right] = e^{-\int_0^t \lambda(X_s)ds} \qquad \textbf{10.4}$$

By inserting (10.3) and (10.4) in (10.1) we obtain

$$Q_t(\tau > T|\tau > t) = 1_{\{\tau>t\}}\mathbb{E}^Q\left(e^{-\int_t^T \lambda(X_s)ds}\middle|\mathcal{G}_t\right)$$

and by the earlier definition of the risk neutral survival probability we write

$$Q(t,T) = 1_{\{\tau>t\}}\mathbb{E}^Q\left(e^{-\int_t^T \lambda(X_s)ds}\middle|\mathcal{G}_t\right) \qquad \textbf{10.5}$$

10.4 Guide to the data appendix

The data appendix consists of three MS Excel files where the analysis has been implemented. The layout of the Excel files are identical; they differ only in reference entity. The guide therefore applies to any one of the three included files. The guide consist of two parts, one to explain the worksheets of the files and one to explain the modules containing the VBA code written to carry out the tasks needed.

10.4.1 Worksheets

The first worksheet named *Spread_CIR* calculates all survival probabilities and discount factors needed to determine the model spread under the CIR model, for a given set of parameters. It is in this worksheet the calibration procedure takes place, through minimizing the sum of squared errors between the model spread and the market spread. The following two worksheets, *Spread_G_OU* and *Spread_IG_OU,* has the same purpose as the first one, but for the Gamma-OU model and IG-OU model respectively.

In the next worksheet, *Parameters,* all the parameter sets obtained in the calibration of all models are contained. The parameter sets selected for further investigation are marked in yellow.

The swaption values and the Monte Carlo errors calculated from the parameter sets in yellow are written to the worksheet *Values*. Cells O1:O3 shows the different time indexes. To the left in the worksheet, the graph containing swaption values from set 1 of each model can be found. Further down in the worksheet, the graphs showing the swaption value as a function of the strike are shown for each model individually.

The relative differences between the swaption values of the parameter sets are calculated in the worksheet *Relative Difference,* while the implied volatilities are calculated in the sheet *ImpliedVol.* Both figures are calculated through custom made functions.

Finally, the worksheet *Path* contains a path generator for the three processes, where the desired parameters can be filled in and a sample path is shown graphically to the right in the worksheet.

10.4.2 Modules

The calibration procedures of the three models each have their own module, *Calibration_CIR, Calibration_G_OU and Calibration_IG_OU,* where the code that implements the looping through different starting values and initiating the minimization process is found. A reference to solver in VBA needs to be made to run the procedures.

The module *Functions* contains the different custom made functions used to calculate different quantities of interest. Namely the CDS value, the Annuity, the Forward Spread, Mean and Standard Deviation of swaption sample values, the Relative Difference, the Black Price of a swaption and the Implied Volatility.

The module *Path* contains the code used for the path generator, and in the module *RandomNumbers* all functions that generate random numbers are found.

Finally, in the three last modules the codes implementing the Monte Carlo Method are found, one for each model.